Author Manuscript

Author Manuscript

Author Manuscript

Author Manuscript

HHS Public Access

Author manuscript

J Control Release. Author manuscript; available in PMC 2021 December 23.

Published in final edited form as:

J Control Release. 2020 June 10; 322: 64–80. doi:10.1016/j.jconrel.2020.03.020.

Renal clearable nanocarriers: Overcoming the physiological barriers for precise drug delivery and clearance

Chuanqi Peng[1], **Yingyu Huang**[1], **Jie Zheng**[*]

Department of Chemistry and Biochemistry, The University of Texas at Dallas, 800 West Campbell Road, Richardson, TX 75080, USA

Abstract

Physiological barriers encountered in the clinical translation of cancer nanomedicines inspire the community to more deeply understand nano-bio interactions in not only tumor microenvironment but also entire body and develop new nanocarriers to tackle these barriers. Renal clearable nanocarriers are one kind of these newly emerged drug delivery systems (DDSs), which enable drugs to rapidly penetrate into the tumor cores with no need of long blood retention and escape macrophage uptake in the meantime they can also enhance body elimination of non-targeted anticancer drugs. As a result, they can improve therapeutic efficacies and reduce side effects of anticancer drugs. Not limited to anticancer drugs, diagnostic agents can also be achieved with these renal clearable DDSs, which might also be applied to improve the precision in the gene editing and immunotherapy in the future.

Keywords

Cancer; Drug delivery; Nanoparticle; Nanocarriers; Nanomedicine; Physiological barriers; Renal clearance

1. Introduction

The concept of “magic bullet” in cancer treatment, proposed initially by Paul Ehrlich over a century ago, compels therapeutic agents in the body to differentiate and target cancerous tissues from healthy ones [1–3]. However, most anticancer drugs in systemic delivery show weak selectivity to tumors but permeate everywhere and destruct both cancer and normal cells, resulting in the limited therapeutic efficacy but severe side effects. During the recent decades, numerous drug delivery systems (DDSs) in nano-scale (10–200 nm) have been developed in order to improve the efficacy and reduce side effects of carried small-molecule drugs compared to conventional free-drug formulations [4–7]. After being loaded on the engineered nanoparticles (NPs) of sizes above kidney filtration threshold

[*]Corresponding author. jiezheng@utdallas.edu (J. Zheng).

[1]Both authors contributed equally.

Declaration of Competing Interest

The authors declare no competing financial interest.

Appendix A. Supplementary data

Supplementary data to this article can be found online at https://doi.org/10.1016/j.jconrel.2020.03.020.

Author Manuscript Author Manuscript Author Manuscript Author Manuscript

(KFT) [8,9] and interendothelial junctions [10] (approximately 6 nm), the carried drugs can circulate in bloodstream for long time by escaping the rapid renal elimination as well as permeation across normal vasculatures, and then accumulate in tumor environment with higher selectivity through the enhanced permeability and retention (EPR) effect [11]. This EPR-based targeting strategy has long been the fundamental principle in the design and practices of NP-based anticancer drug delivery.

Despite high expectations from both researchers and patients for the clinical translation of such concept, cancer nanomedicines suffered a setback in recent years due to the mixed results in clinical investigation and translation. The well-known PEGylated liposomal DDSs (drug-encapsulated liposomes with poly(ethylene glycol), PEG, coating), as the earliest and major type of commercially available nano-formulations in clinics, have been proven to significantly increase the solubility and prolong blood circulation half-lives of loaded drugs for delivery [12,13]. However, a recent meta-analysis on the clinical trials from 1990 to 2015 revealed no significant improvement in patient survival using such PEGylated liposomal formulations (i.e., Doxil) compared to the conventional small-molecule drug, doxorubicin (DOX) [14]. Meanwhile, BIND Therapeutics, one of the leading nanomedicine companies, declared bankruptcy in 2016 due to the disappointing results of its polymeric nanocarriers in clinical trials for active cancer targeting [15]. With more rigorous investigation, Chan et al. discussed and pointed out that few nanomedicines currently entering the clinical phases were emphatically exploiting the newly developed nanotechnology for the effective treatment of solid tumors [16].

The slow clinical translation for many cancer nanomedicines has prompted a revisit of NP-based drug delivery at a more fundamental level [17]. After surveying a variety of cancer-targeting NPs in the past ten years, Chan et al. reported that only 0.7% (median) of the administrated NPs was delivered into solid tumors [18], which set forth the discussion of the “delivery problem” to current nanomedicines [19,20]. In the meantime, many ground-breaking understandings have been accomplished towards the various physiological and pathophysiological barriers to cancer nanomedicines during the in vivo transport and delivery processes [21–23], from the mononuclear phagocyte system (MPS), abnormal tumor vasculature, to tumor microenvironment (TME), etc. These emerging breakthroughs would significantly advance more insights in the strategic design and practice of next-generation nano-DDSs. With increasing fundamental explorations in these physiological barriers, developing novel strategies that can successfully tackle these roadblocks and improve the delivery effectiveness is highly desired for the future clinical translation of cancer nanomedicines [24–26].

Distinct from the current delivery strategies using large-sized nanomedicines, renal clearable NP-based DDSs have recently been developed with unique physiological behaviors: Due to the ultrasmall sizes (< 8 nm), these nanocarriers with ultrahigh vascular permeability enable drug delivery into more population of tumor cells for improved efficacy; meanwhile, the DDSs with sizes near or smaller than the KFT can be eliminated effectively through renal excretion, which significantly reduces DDS uptake by macrophage system (i.e., liver and spleen) and minimizes long-term accumulation of off-target drugs in healthy tissues. These strengths of renal clearable nanocarriers in the in vivo targeting and elimination may

Author Manuscript Author Manuscript Author Manuscript Author Manuscript

address many underlying challenges faced by many currently engineered non-renal clearable nanomedicines. In this review, we briefly overview the critical physiological barriers to current nanomedicines, and more importantly, summarize some newly proposed delivery strategies that could resolve some specific challenges during the circulation, targeting and elimination processes. Then, we introduce the renal clearable NP-based delivery strategy and discuss how these renal clearable nanocarriers can potentially overcome these physiological barriers for precision drug delivery and clearance, allowing for improved therapeutic index by enhancing both efficacy and safety concurrently. We believe that renal clearable DDSs with such unique strengths in drug delivery will offer new opportunities to facilitate the clinical translation of cancer nanomedicines.

2. Physiological barriers and emerging delivery strategies

Nanomedicines are engineered to accumulate in cancerous tissues at high concentrations and selectively interact with cancer cells (Fig. 1A). Upon systemic administration, the engineered DDSs generally take a sequential in vivo transport route towards cancer targeting and treatment, including: 1) circulation in bloodstream, 2) extravasation across tumor vasculature into TME, 3) penetration within tumor interstitial space to reach cancer cells, and 4) internalization by cancer cells (Fig. 1B). While these nanomedicines are expected to have increased tumor targeting, delivery and efficacy, the side-effect and toxicity of off-target therapeutics are mainly governed by the systemic clearance pathway and nonspecific accumulation in other organs (Fig. 1C) [27–29]. During the past decade, the physiological barriers during these in vivo transport processes have been identified and found to significantly limit the delivery effectiveness of a great number of cancer nanomedicines, which has been extensively reviewed by others in detail [5,7,21–23,25,30]. In this section, after briefly introducing the physiological barriers along the systemic delivery route, we dedicate to summarizing the newly emerged delivery strategies (in nanoparticle design and physiological remodeling, Fig. 2) that are intended for overcoming these barriers so as to offer more fundamental understandings and perspectives in the future practice and success of nanomedicines.

2.1. Mononuclear phagocyte system

The MPS represents one of the most important barriers in systemic delivery of nanomedicines [31]. As a part of the immune system, the MPS consists of a class of phagocytic cells (monocytes and macrophages) mainly located in liver, spleen and lymph nodes. Due to the opsonization of NPs via plasma protein adsorption, the administrated nanomedicines in bloodstream may be immediately sequestered by the liver and spleen through phagocytosis, resulting in shortened circulatory half-life in pharmacokinetics and limited tumor targeting [32,33]. Clearance mechanism of nanomaterials by liver has been thoroughly elucidated by Chan et al. in relation to blood flow dynamics, organ microarchitecture and cellular phenotype [34]. The interaction of NPs with liver nonparenchymal cells (e.g., Kupffer cells and sinusoidal endothelial cells) determines the elimination fate [29]. Moreover, the formation of protein corona will dramatically change the physicochemical properties of functionalized NPs (including hydrodynamic diameter,

Author Manuscript Author Manuscript Author Manuscript Author Manuscript

HD, and surface charge), and thus affect the nanoparticle pathophysiological fate [35] and impair the targeting capability of active-targeting ligands (e.g., transferrin) [36,37].

Current strategies to escape rapid MPS uptake and blood clearance emphasize on resisting nonspecific protein binding of nanomedicines to prolong their blood circulation [30]. PEG surface coating or PEGylation has long been recognized as a feasible approach to prevent protein adsorption onto nanomaterials due to the hydration of ethylene glycol and resulting steric hinderance (Fig. 2A) [38–40], in particular, since the FDA approval of PEGylated liposomal doxorubicin (Doxil) for clinical cancer treatment in 1995 [41]. Notably, the effect of PEGylation on blood circulation half-life is closely related to the PEG chain length, core size of NPs and surface PEG density [40,42–44]. In general, blood circulation half-life of NPs increases with the increase of PEG chain length [45,46] or with the decrease of particle core size [47]. Meanwhile, Farokhzad et al. reported that, for PEG-PLGA NPs (55, 90 and 140 nm) with surface PEG (5 kDa) density below ~20 PEG chains per 100 nm^2, blood circulation of NPs increases with the increase of surface PEG density or decrease of particle size [48]. Surprisingly, when the surface PEG density is above this critical value, the NPs exhibit roughly the same blood circulation profiles, irrespective of particle size. However, a follow-up question to this is whether such threshold in surface PEG density for PEG 5 kDa can be applied to the PEG ligands of other chain length. In addition, prolonged blood circulation of nanomedicines can also be achieved by surface coating with other ligands, including zwitterionic ligands, cell membrane, and “self” peptides, etc. Similar to PEG, zwitterionic or mix-charged ligands protect nanomaterials against protein binding due to electrostatically induced hydration [49–53]. Furthermore, Zhang et al. developed polymeric NPs camouflaged by membrane of erythrocytes [54] as well as other cells [55–57], which exhibited 2.5 times longer circulatory half-life compared with PEGylated counterpart. Discher et al. attached a CD47 ‘self’ peptide to virus-size NPs to delay macrophage-mediated blood clearance and enhance delivery to tumors [58]. With most of the research efforts dedicated to NP design, a recent study suggests that depletion of liver macrophages (Kupffer cells) can increase NP delivery to tumors by reducing nonspecific liver uptake and prolonging blood circulation (Fig. 2B) regardless of tumor type, NP size and material [59], which may open a new path to enhance nanomedicine delivery through physiological remodeling.

2.2. Abnormal tumor vasculature

Solid tumors develop tortuous and chaotic neovasculature by yielding excessive proangiogenesis factors such as vascular endothelial growth factor (VEGF) in order to meet their increasing metabolic demands [3,60,61]. Structural abnormalities of tumor vasculature are often characterized as larger junctions between endothelial cells, detached pericytes and abnormally thick or thin basement membrane [62–64]. Such abnormalities permit the enhanced vascular permeability and tumor accumulation of circulating NPs, while the poorly developed lymphatic drainage further retains NPs in TME. This gives rise to the most well-known pathophysiological phenomenon in tumor – the EPR effect [11]. Even though tumor targeting through NP extravasation has been the primary principle in the strategic design of engineered nanomedicines, the pathophysiological features of tumor vasculature also hinder intratumoral transport and drug delivery of nanomedicines [21]. Blood flow rate

Author Manuscript Author Manuscript Author Manuscript Author Manuscript

can be greatly compromised and heterogeneous in tumor vasculature due to the solid stress during tumor growth as well as dysfunctional lymphatic drainage and resulting elevated interstitial fluid pressure (IFP) [65–68]. Jain et al. reported that the IFP uniformly elevates in the tumor core and drops back to normal in the tumor margin [67,69,70]. Additionally, the excessive blood vessel leakiness leads to plasma escape, hemoconcentration, and thus creating blood flow stasis [71–73]. As a result, the elevated IFP and poor blood perfusion in tumors impair NP extravasation into tumor interstitium and delivery efficiency [74]. Due to the elevated IFP and resulting impaired vascular permeability, the hindered intratumoral mass transfer further induces hypoxia and low extracellular pH in TME, causing resistance to radiotherapy and chemotherapy and also increasing chance of tumor metastasis [21].

To understand how to overcome the pathophysiological barrier imposed by tumor vasculature, engineered nanomaterials with distinct physicochemical properties (size, surface charge, shape/geometry and softness, Fig. 2C) have been evaluated. Size dependency in NP extravasation was mostly investigated using engineered non-renal clearable NPs with size range (10–200 nm) above the KFT. These engineered NPs with smaller sizes possess greater vascular permeability, which usually extravasate at faster rates across interendothelial junctions compared to larger NPs [65]. For instance, the 90-nm liposome showed 6 times reduced permeability and much more heterogeneous distribution in human tumor xenograft compared with 6-nm bovine serum albumin [75]. In terms of NP shape, while rod-shape NPs may extravasate faster in tumor than spherical NPs [76], the correlation of permeability with NP shape still varies significantly among different tumor models as reported by Gambhir et al. using quantum dots (QDs) and single-walled carbon nanotubes (SWCNTs) in SKOV-3, U87MG and LS174T tumor models [77]. More recently, Liang et al. reported that the NP softness also plays a critical role in regulating drug delivery efficiency by enhancing the extravasation, penetration and preferential uptake by highly tumorigenic tumor-repopulating cells [78]. In contrast to the EPR-mediated NP extravasation, it is worth noting that many reports also proposed NP extravasation by transcellular transport through endothelial cells [79–82]. When it comes to the transcellular transport mechanism, the cationic NPs can be more effectively taken up by endothelium and therefore penetrate into broad tumor tissues through caveolae-mediated endocytosis and transcytosis [79,83]. While cationic NPs typically exhibit shorter blood circulation, Shen et al. reported the polymer-drug conjugate that changes into positive charge state in tumor vasculature through γ-glutamyl transpeptidase (GGT)-triggered charge reversal to facilitate transendothelial and transcellular transport for the relatively uniform intratumoral distribution [79]. Moreover, coadministration of tumor-penetrating peptide – iRGD with NPs have shown increased vascular permeability for DDS extravasation via neuropilin-1 (NRP-1)-mediated endocytic transport [80,84].

Aside from overcoming abnormal vasculature barrier through NP design, Jain et al. proposed normalization of tumor vasculature through antiangiogenic therapy to alleviate hypoxia by increasing oxygen supply and to enhance the efficacy of conventional therapies as well as immunotherapy [85–87]. Tumor angiogenesis is triggered by the overexpression of proangiogenic factors such as VEGF over antiangiogenic factors such as sVEGFR1 and thrombospondins [86,88]. Administration of anti-VEGF agents (e.g., bevacizumab) helps neutralize the excessive VEGF and remodel tumor vasculature to

Author Manuscript Author Manuscript Author Manuscript Author Manuscript

normal by narrowing the interendothelial junctions and increasing tumor perfusion (Fig. 2D) [89,90]. While the narrowed interendothelial junctions sacrifice vascular permeability, one question that normally arises here is how vascular normalization would improve the efficacy of nanomedicines. With further investigation, Jain et al. demonstrated that vascular normalization favors small therapeutic agents (10-nm Abraxane) rather than large ones (100-nm Doxil) [85]. These combination therapies involved in vascular normalization hold great promise to extend survival of cancer patients as well as to enhance the prospects of developing curative treatment for different cancers [87,90]. On the other hand, some strategies aim to further open up the interendothelial junctions for NP extravasation by using hyperthermia or excess VEGF [91–94], however, some concerns remain such as the increased risk of metastasis due to intravasation of cancer cells into circulation.

2.3. Tumor microenvironment

After extravasation from tumor blood vessels, DDSs need to penetrate through TME in order to reach and interact with tumor cells [74]. There are several characteristics of TME (Fig. 1A): the dense extracellular matrix (ECM), high IFP, hypoxia (due to insufficient oxygen supply) and low extracellular pH (due to deregulated glucose metabolism, also known as the Warburg effect). ECM consists of a cross-linked network of collagen and elastin fibers, proteoglycans and hyaluronic acid. Together these compositions provide structural integrity of solid tumors [95,96]. The presence of dense ECM and high IFP serves as the formidable physical barrier that impedes interstitial transport of nano-DDSs [75,85,97]. Meanwhile, biological barriers, including nonspecific uptake by perivascular stromal cells (e.g., tumor-associated macrophages, TAMs), also limit DDS penetration and targeting to cancer cells [98,99]. Hypoxia is known to not only aid the cancer metastasis and progression [100] but also diminish the therapeutic outcome of various therapies such as chemotherapy, and photodynamic therapy that requires effective activity of oxygen [101–103]. Furthermore, the acidic condition of tumor environment affects penetration of DDSs by changing their overall charge state, affinity to ECM components, as well as further interaction with cancer cells.

Extensive research efforts have been dedicated to enhancing the intratumoral penetration of engineered NPs by tuning their physicochemical properties. Initially, most fundamental understandings focused on the nanoparticle interaction with and penetration (via passive diffusion) in the TME. Within tumor interstitium, NPs with smaller sizes diffuse faster, whereas elongated nanomaterials (i.e., nanorods) may transport more rapidly and distribute more uniformly than spherical NPs (Fig. 2E) [76]. In addition, the neutrally charged NPs penetrate more uniformly than the cationic, ionic or zwitterionic counterparts as a result of less electrostatic hindrance by the charged ECM components (for example, collagen fibers are slightly positively charged, while proteoglycans and hyaluronic acid are highly negatively charged). In contrast to the nanoparticle diffusion in TME, a number of engineered DDSs also enable the transcellular transport throughout tumor tissues via the caveolae/clathrin/receptor-mediated endocytosis and transcytosis [104]. For instance, by taking advantage of the caveolae-mediated transcytosis, cationic or cationized DDSs have been reported to penetrate deeper across multi-layer cancer cells and distribute broadly in the TME [79,105]. In addition, the coadministration of tumor-penetrating peptide (iRGD) enhances the intratumoral penetration of DDSs and free drugs through the receptor

Author Manuscript Author Manuscript Author Manuscript Author Manuscript

(NRP-1)-mediated transport and improves efficacy among multiple tumor models [80,81]. Such transcytosis-mediated extravasation and penetration may offer a viable solution to circumvent the many physical and biological barriers imposed by the abnormal tumor vasculature and hostile TME.

Other approaches to overcome the penetration barriers involve in the strategic design of stimuli-responsive DDSs [106,107]. For example, Shen and Wang et al. reported DDSs that can switch the surface charge from negative or zwitterionic to positive in the acidic TME to increase penetration and enhance cellular interaction [108,109]. Meanwhile, Wang and Nie et al. developed pH-responsive clustered NPs (100 nm) that discharge ultrasmall DDSs (platinum prodrug-conjugated dendrimers, ~5 nm) in acidic TME for the enhanced intratumoral delivery [110]. Moreover, Gao et al. reported the transistor-like ultra-pH-sensitive (UPS) NPs that utilize a pH-triggered disassembly mechanism and thus enable precision tumor detection and potential delivery [111]. Similar to the acidic pH condition, tumor hypoxia can also be considered as validated target via the approaches including bioreductive prodrugs and inhibitors of molecular targets upon which hypoxic cell survival depends [101].

Physiological remodeling of TME has also been proposed to enhance the penetration of DDSs during the recent two decades. Matrix modifiers, such as bacterial collagenase, relaxin, and matrix metalloproteinases (MMP-1 and MMP-8), have been investigated to degrade the collagen or proteoglycan networks (Fig. 2F) and to improve the convection and efficacy of intratumorally injected therapeutics (oncolytic viruses) [112–114]. Other strategies to enhance NP penetration include dilating the pores of ECM by co-infusion of NPs with hyperosmolar mannitol solution or hypertonic buffer solution [115] and pre-treating tumor with hyaluronidase [116]. However, these agents also induce normal tissue toxicity (for the bacterial collagenase) or increase the risk of tumor progression (for relaxin, MMPs, and hyaluronidase). Later, losartan, a clinically approved angiotensin II receptor blocker (ARB), was investigated and found to improve the intratumoral penetration and efficacy of systemically administered nanotherapeutics to highly fibrotic solid tumors such as pancreatic adenocarcinomas [117]. It would be meaningful to further understand how these enzymatic modifiers fundamentally affect the targeting, transport and retention of administrated DDSs as well as their interactions with tumor cells.

2.4. Cellular internalization

Many nanomedicines are intended to actively target cancer cells for effective cell-specific treatments (i.e., genome editing, peptide inhibitors and nucleic acid therapies), however, these active-targeting therapeutics entering the tumor environment are often hindered considerably not only due to the ECM barrier but also due to the massive uptake by non-cancer cells. The solid tumors are known to consist of multiple cell types, including cancer cells, and non-cancer cells such as endothelial cells, pericytes, fibroblasts, TAMs, and immune cells. A recent study by Chan et al. reported that less than 14 out of 1,000,000 intravenously administrated active-targeting NPs were delivered to the targeted cancer cells in tumor, and only 2 out of 100 cancer cells interacted with these NPs, as a result of acellular regions and TAMs serving as the greatest intratumoral barriers [99]. Another study

Author Manuscript Author Manuscript Author Manuscript Author Manuscript

by Huang et al. also found 7 times higher uptake of NPs by tumor-associated fibroblasts compared to other cells including cancer cells [118]. These quantitative results suggest that fundamental understanding on the cellular interaction and intratumoral fate of DDSs is critical to future nanomedicine design for therapeutic improvement. Meanwhile, the quantitative analysis and correlation of targeting efficiency with therapeutic efficacy are also demanded in order to evaluate the performance and potential for different delivery strategies [119]. Other biological factors such as vesicular and organellar barriers and drug efflux transporters have been thoroughly reviewed elsewhere and will not be discussed in detail here.

To overcome the final biological barrier that governs the cellular interaction of nanomedicines, various delivery strategies have been investigated at in vitro or in vivo level with regards to the nanoparticle design and physiological remodeling as well. The underlying critical objective is to enhance the affinity of NPs towards cancer cell membrane. A viable approach is the active targeting by modifying DDS surface with targeting ligands that specifically bind to the overexpressed receptors on specific cancer cells, for example, cRGD peptide, anti-human epidermal growth factor receptor 2 (HER2), single-chain variable fragments (scFv). Meanwhile, the engineered NPs not only work as simple carriers but also play an active role in mediating biological effects: an optimal size of about 50 nm has shown the greatest efficiency for cellular uptake of NPs [120], whereas more hydrophobic and positively-charged NPs hold higher affinity in cell-membrane penetration and internalization (Fig. 2G) [121]. Other strategies to overcome such cellular barrier focus on remodeling the cellular environment of solid tumors by eliminating the competing nanoparticle internalization from non-cancer cells (i.e., TAMs, fibroblasts, Fig. 2H). The depletion of TAMs using clodronate liposomes has been investigated with significant inhibition of tumor progression, angiogenesis and metastasis in the preclinical studies [122–124]. Furthermore, Olive et al. discovered that depleting tumor-associated stromal tissue by inhibiting the Hedgehog cellular signaling pathway can also enhance the efficacy of chemotherapy [125].

3. Renal clearable delivery strategy

3.1. Renal clearable NPs for cancer targeting

3.1.1. Renal clearable NPs—While increasing number of engineered NPs have been investigated as potential nanocarriers for cancer therapy, the elevated liver accumulation and retention (30–99% of the injected NPs) remains one formidable challenge for most administrated NPs, especially for the inorganic, non-degradable or so-called hard nanomaterials [27,28,34]. In contrast to the nanoparticle uptake in liver macrophage and resulting slow hepatic clearance, the renal excretion through kidney filtration may offer a much more effective clearance pathway for the ultrasmall sized NPs. With more precise determination of the KFT [9,126], the administrated NPs of size (in HD < 10 nm) near or below the KFT can be renally clearable at high efficiency. In general, the renal clearable NPs are these administrated NPs that particularly have the renal clearance efficiency of more than 50% injection dose (ID) within a short period of time (i.e., 48 h post-injection, p.i., Table S1). This is of great significance to minimize the body accumulation and long-

Author Manuscript Author Manuscript Author Manuscript Author Manuscript

term exposure of hazards for safety regulation compared to the non-renal clearable NPs of larger size. During the past decade, many renal clearable ultrasmall NPs have been developed. Some representative NPs are shown in Fig. 3A–G, as well as Table S1 in supplementary information [9,53,127–141], including the quantum dots (QDs), silica NPs (C-dots), carbonaceous dots, polymeric NPs (H-dots), PEGylated conjugates/NPs as well as noble metal (such as gold and silver) nanoparticles or nanoclusters (NCs), etc. With more investigation, such efficient renal clearance has been found to attribute not only to the ultrasmall NP size for renal glomerular filtration but also to a passivated zwitterionic or PEGylated surface coverage so that the serum protein adsorption and resulting MPS uptake of NPs can be significantly minimized [9,51,53]. To be noted, renal elimination can also be achieved with small-molecule probes [142,143], biodegradable nanomaterials [144–147], as well as several large nanomaterials such as the single-walled or multi-walled carbon nanotubes (SWCNTs or MWCNTs, respectively, Fig. 3H and I) [129,148].

Moreover, a myriad of renal clearable NPs have been used in the tumor targeting and imaging and found significantly improved tumor selectivity or tumor-to-background ratio [53,149]. Firstly, this is fundamentally because these ultrasmall NPs can rapidly extravasate, distribute and retain in tumor tissues due to their high permeability in tumor vasculature and microenvironment [119,150]. By comparing the nanoparticle distribution in blood, tumor as well as background tissues, more evidences suggest that the ultrasmall NPs can outperform larger NPs in the transvascular and interstitial transport in various types of tumors [53,85,119,149,150], even though the proposed EPR effect initially favors non-renal clearable NPs for high tumor accumulation from the conventional view point [6,11]. Secondly, the improved tumor selectivity also results from the rapid elimination of renal clearable NPs from healthy tissues as well as bloodstream, which greatly decreases the background signals for enhancing tumor contrast [53,149,151]. Since rapid renal elimination of NPs considerably reduces the body accumulation and potential toxicological concerns, renal clearable C-dots have been evaluated in the clinics as multi-modality probes for cancer imaging [152] and renal clearable AuNPs have been investigated in non-human primates for potential disease diagnosis and clinical translation in future [153].

3.1.2. Passive and active targeting of renal clearable NPs—Renal clearable NPs have shown great potential in the cancer diagnosis due to their increased tumor selectivity by the rapid intratumoral diffusion, tumor retention and also efficient background elimination. Nonetheless, these NPs are generally not considered as suitable candidates to deliver anticancer drugs into solid tumors at sufficient concentration compared to conventional non-renal clearable NPs, which are typically of increased nanoparticle dimensions for the prolonged blood circulation. This is mainly because these ultrasmall NPs cannot retain in bloodstream for long time for further accumulation in tumor tissues based on the abovementioned EPR effect. Therefore, a fundamental challenge for these renal clearable NPs is whether they can actually accumulate in tumor site at sufficient concentration for drug delivery. To answer this question, we summarized some representative renal clearable NPs in the literature for both passive and active tumor targeting (Tables S1 and S2 in supplementary information, respectively) and plotted these results in Figs. 4 and 5. The “renal clearable” NPs would typically have the efficient renal clearance of more than 50%

Author Manuscript Author Manuscript Author Manuscript Author Manuscript

ID in the short term (i.e., 48 h p.i.), as shown in Fig. 4. Meanwhile, other NPs reported with a lower renal clearance efficiency (10–50% ID) was denoted as “insufficiently renal clearable”, which was also summarized here for a more comprehensive comparison and analysis. As a result, the engineered NPs with more efficient renal clearance (> 80%ID) would indeed have a lower efficiency in passive targeting (< 3%ID/g, Fig. 4). This is understandable because the more rapid renal elimination will drastically decrease the blood retention of NPs and resulting tumor accumulation. Therefore, a tradeoff exists between the tumor targeting and renal clearance for these ultrasmall NPs at the range of kidney filtration threshold (~6 nm), where the renal clearable NPs can have the enhanced tumor targeting while maintaining high efficiency of body elimination. Such small size EPR effect has also been discussed recently by Choi et al. by using polymeric NPs, which shows the polymeric NPs (< 12 nm) can achieve enhanced tumor-to-background ratio by both improved EPR-based tumor targeting and efficient renal clearance [154]. In addition, renal clearance can also be affected by the difference in particle shape and flexibility in physiological environment: NPs that are rigid and globular structured have the KFT at about 6 nm, whereas, the NPs that are flexible and linear shaped such as PEG chains remain renal clearable at 12 nm in HD [154,155]. In contrast to the prevailing renal clearable NPs, we reported that the 5.5 nm renal clearable PEGylated gold nanoparticles (PEG-AuNPs) can exhibited significantly higher tumor targeting efficiency (to MCF-7 human breast adenocarcinoma xenograft) with above 8%ID/g from 1 to 12 h post-injection (asterisk (*) in Fig. 4) [51], which may attribute not only to PEGylated surface coating for prolonging circulation but also to the stronger margination effect in the tumor blood flow for the NPs with greater density (i.e., AuNPs vs AgNPs) [156] and resulting NP extravasation. Therefore, such NPs with both high targeting and renal clearance may serve as desirable renal clearable nanocarriers for the passive tumor targeting and effective drug delivery.

In addition to the passive targeting, renal clearable NPs may also target tumors at high selectivity via the active targeting strategy. This has been achieved by these ultrasmall NPs with conjugation of specific targeting moieties to many cancer-specific receptors or antigens so that the targeted renal clearable NPs can interact with these cancer cells via molecular recognition (i.e., ligand-receptor, antigen-antibody interactions). During recent years, Bradbury et al. have successfully used renal clearable C-dots (or C′-dots) to target a variety of in vivo tumor models by exploiting this active targeting strategy, which involved in the targeting of α_v integrin [157,158], melanocortin-1 receptor (MC1-R) [159], prostate-specific membrane antigen (PSMA) [160] and human epidermal growth factor receptor 2 (HER2) [161]. In the meantime, Zhang et al. reported that renal clearable manganese-doped iron oxide NPs conjugated with monocyclic peptides could target the tumors with overexpression of CXC chemokine receptor 4 (CXCR4) at high efficiency (~15.9%ID/g) in the presence of an external magnetic field [162]. As a result, with the targeted strategy, the renal clearable NPs have achieved much higher targeting efficiency (2.6-fold increase, median, Fig. 5) among many cancer types compared to the non-target ones, which allows for the enhanced tumor targeting for those NPs even with the more rapid body elimination (~80%ID). Among these reported active targeting strategies, two studies were involved in the comparison of NPs with targeted and non-targeted conjugating ligands, such as cRGDY vs cRADY, and monocyclic peptides (MCP) vs PEG (where there

Author Manuscript Author Manuscript Author Manuscript Author Manuscript

was 0.7 nm difference in HD between the two NPs, Table S2) [152,162]; Meanwhile, other four studies investigated the active targeting efficiency of targeted NPs to tumors with both overexpressed and underexpressed receptors [157,158,160,161]. In addition, another one study used the co-injection of inhibitor in order to understand the targeting of the engineered nanocarriers [159]. In contrast to the active targeting via specific receptors, we recently reported that renal clearable AuNPs may serve as novel probes to target tumor acidity due to the differences in surface chemistry and tumor retention of NPs [163]. These results have greatly advanced our understandings in the use of renal clearable NPs for tumor targeting and potential drug delivery.

3.2. Emerging renal clearable DDSs

Many ultrasmall NPs have emerged with efficient renal clearance and have been applied to cancer diagnosis and imaging, however, only few reports have been accomplished to fundamentally understand the in vivo transport and drug delivery of the renal clearable nanocarriers, including AuNPs, C′-dots and H-dots. With extensive investigation, these renal clearable DDSs have been found to behave uniquely in the in vivo transport processes and can overcome a series of physiological barriers for the precision delivery and clearance. In 2016, Choi et al. proposed the renal clearable theranostic organic nanocarriers (H-dots, < 5.5 nm, Fig. 6A) for early tumor detection and potential drug delivery, where these organic nanocarriers (especially with the zwitterionic surface chemistry) exhibited drastically reduced nonspecific background uptake and efficient renal excretion (> 80%ID in 4 h) [53,164]. By exploiting the widely used anticancer drug, DOX, as model, we developed the renal clearable AuNP-based DDS (DOX@AuNPs, ~5 nm, Fig. 6B) and investigated its targeting and elimination profiles based on both the delivery vector and loaded drugs. We discovered that the diverse in vivo transport behaviors of the renal clearable DOX@AuNPs, rapid tumor targeting and efficient renal elimination, may reconcile the long-standing paradoxes between targeting and elimination to many underlying nanomedicines [151]. Shortly after a head-to-head comparison in the intratumoral delivery between the 5 nm renal clearable and 30 nm non-renal clearable AuNP-based DDSs (namely DDS-5 and DDS-30, respectively), we reported that ultrahigh vascular permeability of the renal clearable DDS-5 plays a more critical role in tumor accumulation, efficacy and therapeutic index of anticancer drugs, allowing for the effective delivery with renal clearable nanocarriers [119]. In the meantime, Bradbury et al. used renal clearable C′ dots (~7 nm) to delivered a small molecular inhibitor (SMI), gefitinib (an epidermal growth factor receptor tyrosine kinase inhibitor), to a non-small cell lung cancer (NSCLC) model [165,166], which showed favorable pharmacokinetics, high drug loading and efficacy, low off-target toxicity compared with free drug. More recently, they also used the targeted C′ dots (Fig. 6C) to investigate the delivery and penetration of another SMI, dasatinib, to high-grade malignant brain tumor model [167], which led to the initiation of a Phase 1 clinical trial in the glioma targeting. The unique features in minimizing the background accumulation via renal elimination may successfully improve the safety of these nanocarriers. In addition, some other therapeutic modalities in the use of renal clearable NPs have also been investigated, such as photothermal therapy [134,136,140], photodynamic therapy [137,168], and image-guided radiation therapy [138,169]. Moreover, Overholtzer et al. reported that ultrasmall PEG-coated silica NPs (< 10 nm) functionalized with melanoma-targeting peptides could

Author Manuscript Author Manuscript Author Manuscript Author Manuscript

induced the ferroptosis in starved cancer cells and cancer-bearing mice, suggesting the therapeutic potential [170].

3.3. Precision delivery and clearance of renal clearable DDSs

It is known that delivery and efficacy of nanomedicines can be greatly affected by the many physiological barriers during the in vivo transport processes. Different from the many conventional DDSs which are typically non-renal clearable, the renal clearable DDSs have found some unique in vivo transport behaviors. These intriguing features may facilitate the precision delivery and clearance with renal clearable DDSs by overcome these underlying physiological barriers, which are concluded in detail as below:

3.3.1. Altered clearance route with prolonged blood circulation—By introducing a passivated surface coating using PEGylation or zwitterionization, renal clearable NPs can prevent protein adsorption and thus minimize MPS uptake, which allows for the enhanced physiological stability and altered clearance to renal pathway. Meanwhile, most small-molecule drugs for cancer treatment show high affinity to protein binding and rapid hepatobiliary elimination, which results in poor pharmacokinetics but acute hepatotoxicity. Then a fundamental question to these renal clearable nanocarriers is whether they can minimize protein binding of the loaded anticancer drugs for the altered renal clearance as well as improved pharmacokinetics. By loading DOX onto AuNPs, we recently reported that the renal clearable 5 nm DOX@AuNPs, or DDS-5, showed no observable binding to human serum albumin (HSA) and retained a renal clearable size in the physiological conditions [151]. As a result, the DDS-5 can indeed reduce the serum protein binding of loaded DOX and carry the untargeted DOX to be efficiently cleared into the urine. After analysis, renal clearance of DOX (22%ID) for the administrated renal clearable DDS-5 increased to 3.6 and 6.5 times higher than those of free DOX and non-renal clearable DDS-30, respectively, at 24 h p.i. In addition, blood DOX retention of DDS-5 (63.7%ID·h/g, 48-h AUC, area under the curve) was still nearly 10 times higher than that of free DOX (7.7%ID·h/g), which was because the renal clearable nanocarriers reduced serum protein binding of drug and its hepatobiliary elimination. Therefore, in addition to the efficient renal elimination, renal clearable DDS can also increase the tumor targeting of loaded drug by 5 times (to 4.1%ID/g at 12 h p.i.) due to the significantly prolonged blood circulation compared to the free drug (DOX, with tumor targeting of 0.8%ID/g).

3.3.2. Enhanced intratumoral transport with ultrahigh vascular permeability —In addition to the prolonged blood circulation, renal clearable DDSs have possessed strengths in the intratumoral transport kinetics due to the ultrasmall NP sizes. The vascular permeability and intratumoral diffusion coefficient of NPs improve with the decreased NP size, which has been extensively investigated for the various NPs in the non-renal clearable size range (10–200 nm) [21,85,97,150,171]. By systematically comparing the 5 nm renal clearable DDS-5 and 30 nm non-renal clearable DDS-30, we recently reported that the ultrasmall DDS-5 exhibited much higher vascular permeability in the extravasation process and penetrated deeper in the TME. These renal clearable DDS-5 can efficiently diffused into the central areas of tumor environment between two nearby tumor blood vessels and also distributed nearly evenly within the whole tumor from peripheral into tumor core areas

Author Manuscript Author Manuscript Author Manuscript Author Manuscript

[119]. As a result, we observed that the DOX carried by ultrasmall DDS-5 extravasated from tumor vasculature and penetrated deeply into interstitial space within short time (12 h, Fig. 7A); whereas, majority of DOX delivered by large-sized DDS-30 were confined within or near the blood vessels, consistent with previous observations. With further analysis of tumor cells interacting with DOX across different distance from tumor vasculature (Fig. 7B–D), we found that the percentages of tumor cells interacting with DOX for the DDS-5 (36–54%) were 2–5 times more than those of the larger DDS-30 (9–19%). In addition, with increased distance-to-vessel (from 30 to 120 μm), the smaller DDS-5 showed greater difference from larger DDS-30 in the delivery efficiency to tumor cells (increasing from 2.8 to 4.7 times, Fig. 7D). Therefore, renal clearable DDS-5 can achieve about 7 times increase in therapeutic efficacy compared to non-renal clearable DDS-30 under the same dose schedule [119], which was primarily due to the ultrahigh vascular permeability for more effective intratumoral drug delivery. In the meantime, this ultrahigh intratumoral penetration of ultrasmall nanocarriers have also been found in the dendrimer NPs: By analyzing the penetration depth of different sized dendrimers in multicellular tumor spheroids (MCTS), Hong et al. reported that the smaller dendrimers (G2-NH_2, 2.9 nm in diameter) penetrate 2.5 folds deeper than the larger dendrimers (G7-NH_2, 8.1 nm) [172]. In addition, these renal clearable nanocarriers also showed enhanced transvascular and interstitial transport in the tumors with poor permeability, including central nervous system (CNS) tumors as gliomas. Previously, we reported that the 3 nm renal clearable AuNPs can increase the targeting efficiency and specificity to orthotopic murine gliomas by 2.3 and 3.0 times, respectively, compared to 18 nm non-renal clearable counterpart [173]. More recently, Bradbury et al. reported 7 nm renal clearable targeted C′-dots can achieve favorable tumor diffusion and retention in high-grade gliomas as well [167]. These results have greatly advanced our understandings on the nanoparticle transport and drug delivery using renal clearable DDSs in different tumor models or various types of tumor microenvironment.

3.3.3. Improved efficacy among multiple tumor models—Renal clearable nanocarriers increase tumor targeting and drug delivery in a more rapid and effective fashion, because they can minimize MPS uptake, and in the meantime, extravasate into tumor environment with ultrahigh permeability and reach more population of cancer cells [119]. During the past years, a variety of renal clearable NP-based DDSs have been reported with significantly improved efficacy as a result of their unique in vivo transport behaviors [119,151,165,167]. We investigated and compared the antitumor efficacy of AuNP-based renal clearable DDS-5 and non-renal clearable DDS-30 as well as free DOX among different breast cancer models, including a well-established human MCF-7 xenograft (Fig. 8A and B), the human triple-negative breast cancer MDA-MB-231 xenograft, and primary and metastatic (lung) murine 4T1 tumors [119,151]. By precisely tuning the targeting efficiency and vascular permeability, the renal clearable DDS-5 improved the therapeutic efficacy (by evaluating the efficacious dose, ED, of the different formulas) about 7 times to the MCF-7 tumor model, compared with non-renal clearable DDS-30 and free DOX [119]. In addition, this renal clearable DDS-5 showed significant inhibition not only to primary murine 4T1 breast cancer (Fig. 8C and D) but also to its metastasis in lung tissues, which successfully decreased the surface lung nodule counts to 12.9 and 15.7 times of those of DDS-30 and free drug, respectively (Fig. 8E–G). More recently, Bradbury et al. used the targeted C′-dots

Author Manuscript Author Manuscript Author Manuscript Author Manuscript

to deliver the SMIs, and demonstrated enhanced delivery and therapeutic efficacy over that of the free drugs in murine xenograft models of non-small cell lung cancer [165] and the genetically engineered mouse model of glioblastoma [167]. These results suggest that the ultrasmall renal clearable nanocarriers may serve as effective delivery vectors for the treatment of various primary solid tumors, metastatic tumors as well as the poorly permeable tumors.

3.3.4. Minimized off-target and systemic toxicity—Along with the improved efficacy, nanomedicines that are off-target need to be cleared from the body in a reasonable time period without inducing adverse effects from either the delivery vectors or loaded therapeutics. However, most of the administrated non-renal clearable nanocarriers, even including the stealth NPs of prolonged circulation, often have the elevated MPS accumulation (30–99% of the injected dose) over time and then undergo long-term exposure as hazards during the elimination process [28,29]. This would be one of the greatest concerns for the clinical translation of these large, especially, non-biodegradable DDSs due to their body retention and potential toxicity. In contrast, renal clearable nanocarriers not only deliver drugs rapidly with significant tumor inhibition, but also minimize the whole-body accumulation of the off-target drugs due to the altered elimination pathway into renal excretion. By analyzing the biodistribution of the renal clearable DDS-5, non-renal clearable DDS-30 as well as free DOX, we reported that the renal clearable DDS-5 can significantly decrease the accumulation of both NPs and loaded drug not only in the kidney, liver and spleen, but also in heart, lung, and background tissues [119,151]. As a result, the toxicity of renal clearable DDS-5 to these tissues can be greatly minimized compared with non-renal clearable counterpart and free drug. More specifically, free DOX induced the acute impairment to liver and kidney functions, from blood chemistry analysis (Fig. 9A–D) [151]; whereas, non-renal clearable DDS-30 showed the elevated accumulation and retention in liver, spleen and kidney [119]. In contrast, the renal clearable DDS-5 can minimize the interaction of both delivery vector and drug with these tissues, which contributes to the accelerated body elimination and reduced drug-induced toxicity. Even though the renal clearable DDS has smaller size than interendothelial junctions and remains highly permeable across normal vasculature, our recent results showed that the renal clearable DDS not only minimized the drug accumulation into either heart or lung but also accelerated the drug elimination from these background tissues at much faster kinetics (Fig. 9E and F). These findings clearly indicated that the renal clearable nanocarriers may successfully minimize the interaction of loaded drug with healthy tissues and accelerate body elimination of off-target drug. In order to quantitatively understand the improved efficacy and safety, we also evaluated the therapeutic index (TI, equals to the toxic dose/ efficacious dose, TD/ED) of the renal clearable DDS-5 as well as DDS-30 and free DOX. As a result, we found that the renal clearable DDS-5 increases the TI of DOX by one order of magnitude (with 6.7 times increase in ED and 1.5 times decrease in TD), in contrast to the non-renal clearable DDS-30 and free DOX [119]. Therefore, these renal clearable DDSs with both enhanced tumor targeting and body elimination can significantly improve the efficacy and safety of loaded drugs concurrently, offering new opportunities to nanomedicine translation in the future.

Author Manuscript Author Manuscript Author Manuscript Author Manuscript

3.3.5. Delivering molecular agents beyond anticancer drugs—By rational design, renal clearable nanocarriers with the unique physiological behaviors may modulate the in vivo transport and delivery of various types of molecular agents in addition to therapeutic drugs. More recently, we discovered in our lab that the engineered renal clearable nanoprobe responds to the physiological environment (i.e., glutathione-mediated liver detoxification) distinct from molecular imaging agent (as well as non-renal clearable nanoprobes), which further enhances tumor selectively of the carried imaging agent significantly [174]: By conjugating the clinically available fluorescence molecular probe, indocyanine green (ICG), onto the renal clearable glutathione (GSH)-coated Au_{25} NCs to prepare the thiol-activatable fluorescent gold nanoprobe (ICG_4-GS-Au_{25}), we reported that this novel nanoprobe achieved significantly altered blood retention, improved tumor selectivity and body clearance by taking advantage of both the ICG-induced serum protein interaction and GSH-mediated biotransformation during blood circulation. As a result, the ICG_4-GS-Au_{25} not only enhanced tumor accumulation of both delivery vector (GS-Au_{25}, by 2.3 times to 5.4%ID/g) and carried molecular probe (ICG, by 27 times to 4.1%ID/g) but also increased the tumor retention time of ICG signal for two weeks. From the microscopy imaging of tumor tissue with 24 h post-intravenous treatment of ICG_4-GS-Au_{25}, strong ICG near-infrared fluorescence signals were found within a large cell population in tumor environment (Fig. 10). More specifically, the ICG molecules were mainly located in the intracellular endosome-like membrane-bound compartments, indicating the effective delivery of these molecular probes. The results suggested that the physiological barriers in nanomedicine translation, such as liver detoxification, can be turned into a bridge towards maximizing targeting and minimizing toxicity by exploiting such engineered renal clearable NP-based nanoprobes.

4. Conclusion and outlook

Fundamental understandings of the physiological challenges to cancer nanomedicines will advance the more effective and tenable delivery strategies, which underlies the future success in nanomedicine translation into clinics. During the past years, diverse strategies have emerged with potential to overcoming the many physiological barriers through nanoparticle design and physiological remodeling. Distinct from the current delivery strategies, the renal clearable NP-based DDSs with unprecedent in vivo behaviors may effectively overcome the various physiological barriers for the precision drug delivery and clearance. In this review, we systematically discuss the tumor targeting and clearance of renal clearable nanocarriers, as well as summarize the fundamental breakthroughs in the transport and elimination processes of the engineered renal clearable nanocarriers. In the meantime, we also want to specify that there are still some critical points that need to be extensively explored or addressed in the near future before the any possible clinical translation and practice of such renal clearable nanomedicines:

- *To continually improve delivery by precisely tuning the targeting and clearance.* While renal clearable DDSs enhance tumor targeting, intratumoral transport as well as body elimination without the need of long blood circulation, the next question is whether the targeting and clearance of these DDSs can be further precisely tuned by improving the blood circulation. The NP size serves as one

Author Manuscript Author Manuscript Author Manuscript Author Manuscript

major factor governing the blood circulation of engineered NPs, therefore, we prepared the PEG-AuNPs with sizes (from 5.5 to 7.5 and 9.5 nm in HD, with surface coating of PEG 800 Da) slightly above the KFT for the prolonged blood retention. Upon the intravenous injection, these AuNPs showed decreased renal clearance (from 50.9 to 9.8%ID in 24 h) with the increased HD from 5.5 to 9.5 nm (Fig. 11A) due to the decreased kidney filtration for larger NPs. As a result, these AuNPs exhibited a sharp increase in the blood circulation (based on 24-h AUC, Fig. 11B) from 42.7 to 445.5%ID·h/g, with 10 times or 1 order of magnitude increase in such a narrow size range (~6 nm). Surprisingly, the 9.5 nm AuNPs achieved the comparable pharmacokinetics with 90 nm PEGylated liposomes, indicating the long blood circulation can be achieved with ultrasmall nanocarriers as well. Notably, the 9.5 nm AuNPs showed the particle size nearly one order smaller than the 90 nm liposome, which was more favorable for the transvascular and interstitial transport in tumor tissues. Next, we investigated the 9.5 nm cisplatin-loaded AuNPs (Pt-DDS-9.5) and found that the tumor targeting efficiency significantly increased to 9.6%ID/g (AuNPs) at 12 h post-injection, which was 1.7 times higher than the renal clearable DDS-5. As a result, 6.2%ID/g of loaded cisplatin was successfully delivered into tumor tissues, and more importantly, there remained high drug concentration (14.4% ID/g) in blood for tumor accumulation and retention in long term (Fig. 11C). These results indicate that, by changing the DDS size within this narrow range (5–10 nm), both tumor targeting and renal elimination can be precisely tuned with the engineered renal clearable nanocarriers.

- *To deliver anticancer drugs with greater potency and loading stability.* The renal clearable nanocarriers can significantly increase the tumor selectivity or tumor-to-background ratio by not only delivering drugs into tumor tissues at high concentration but also minimizing the body accumulation of off-target drugs. This will contribute to an improved therapeutic index by the both enhanced efficacy and safety. However, the conventional anticancer drugs, such as doxorubicin and cisplatin, are only of the modest potency, which normally have the IC_{50} (half maximal inhibitory concentration) to cancer cells at the micromolar (μM) scale and above [151]. Therefore, future studies may involve in the screening of the highly potent therapeutics, especially the anticancer agents with the IC_{50} near or below nanomolar (nM) level, for the drug loading and cancer treatment with these nanocarriers of high tumor selectivity. More importantly, the extensive investigations should also be carried on to further improve the loading stability of highly potent drugs and physiological stability of the DDSs.
- *To deliver large molecules and proteins.* Due to the ultrasmall size of renal clearable NPs, very few studies have been conducted to deliver the large molecules or proteins (> 5 kDa) using these ultrasmall nanocarriers. While it is known that the large volume of the carried molecules will significantly alter the physicochemical and physiochemical properties, the careful selection of the cargoes and systematical in vivo investigation are required for the successful

Author Manuscript Author Manuscript Author Manuscript Author Manuscript

delivery. For example, we previously conjugated a monomeric insulin (5.3 kDa) onto renal clearable AuNPs at insulin-to-AuNP ratio of 1: 1 and investigated the in vivo profile, function and bioactivity of the delivery system [175]. It is also worth noting that the Au—S bonding may make it accessible to conjugate thiolated large molecules (such as small-interfering RNAs, ~13 kDa) using these renal clearable AuNPs, AuNCs or Au—S (gold-sulfur) polymers.

- *To evaluate and improve the biosafety of renal clearable nanocarriers.* Renal elimination of the administrated nanomedicines may significant minimize the accumulation and long-term retention of off-target therapeutics in vital organs and tissues. Due to the efficient glomerular filtration and minimized interaction in renal tubule structures, renal clearable nanocarriers (i.e., AuNPs) have one of the fastest elimination rates in kidney (Fig. 12). However, it will take much longer time for other organs (liver, spleen, heart, etc.) to eliminate these NPs, which remains as a major safety issue to many renal clearable nanocarriers, especially, to these hard nanomaterials. Therefore, it is necessary to not only minimize the interaction and accumulation of these nanocarriers in healthy tissues but also evaluate the short-term and long-term biosafety of the emerging nanocarriers systematically. For instance, renal clearable AuNPs have been investigated with the no-observed-adverse-effect level (NOAEL) more than 1000 $mg{\cdot}kg^{-1}$ in mice and 250 $mg{\cdot}kg^{-1}$ in non-human primates (cynomolgus monkeys) [153]. A high biocompatibility of these renal clearable NPs would significantly minimize the safety concern and also increase their potential in the future clinical practices.
- *To combine emerging therapies with renal clearable nanocarriers.* The emerging therapies, such as immunotherapy, gene editing and gene therapy, have demonstrated unprecedent successes in the clinical treatments of cancers as well as rare disease like genetic disorders. However, for the broad implementation of immunotherapies, the key challenge remains as the controlled modulation (activation or suppression) of immune cells [176], including lymphocytes, macrophages, dendritic cells, natural killer (NK) cells, cytotoxic T lymphocytes (CTL), etc., which is because many therapeutics have shown serious adverse effects such as autoimmunity and nonspecific inflammation. Therefore, it is critical to not only enhance targeting and therapeutic efficacy but also effectively alleviate the adverse effects. Recently, Zhang et al. showed that particle size (for NPs of 5–15 nm) may affect the antigen retention and presentation in lymph nodes, indicating the humoral immunity may be simply manipulating the NP size to produce effectiveness of immunomodulation [177]. While it has shown that larger NPs may retain in lymph node for longer time, the ultrasmall renal clearable nanocarriers may potentially serve as rapid targeting therapeutics after the rational design. Meanwhile, gene therapy is the delivery of nucleic acids as therapeutics into the target cells to treat disease. The most clinically relevant gene therapies often involve in the use of virus delivery vectors such as adeno-associated viruses (AAVs) and lentiviruses, whereas the technology of CRISPR-based gene editing therapy (i.e., CRISPR/Cas9 system) has opened new

Author Manuscript Author Manuscript Author Manuscript Author Manuscript

paths to mediating genome engineering with high precision. We believe, with more extensive investigation, the renal clearable nanocarriers may achieve more fundamental understandings in the delivery of nucleic acids or gene-editing tools and related applications [178].

The comprehensive understanding of the above challenges will substantiate the versatile medical potentials of these renal clearable nanocarriers. To be noted, it is also critical to pay attention to the body's high sensitivity towards the physicochemical properties of nano-DDSs, since our findings suggest that seemingly small variations among these nanomaterials can result in significant differences in the nano-bio interactions and also in vivo transport behaviors. For example, we recently observed that the seven-atom decrease in particle size in the sub-nm regime may enhance the nanoparticle interactions with the glomeruli and slow down their renal filtration [179]. Therefore, it is important to precisely control the physicochemical properties of these nanomedicines, reduce heterogeneity and increase reproducibility [180]. With the joint efforts in the field, we believe the physiological understandings and therapeutic potentials of these nanomedicines can be greatly advanced, which will eventually contribute to the attainable clinical practice and success in the near future.

Supplementary Material

Refer to Web version on PubMed Central for supplementary material.

Acknowledgements

This study was supported by the NIH (1R01DK103363), CPRIT (RP200233), and Welch Research Foundation [AT-1974-20180324 (JZ)], and Cecil H. and Ida Green Professorship (JZ) from The University of Texas at Dallas.

References

[1]. Chabner BA, Roberts TG, Chemotherapy and the war on cancer, Nat. Rev. Cancer 5 (2005) 65–72, 10.1038/nrc1529. [PubMed: 15630416]

[2]. Bae YH, Park K, Targeted drug delivery to tumors: myths, reality and possibility, J. Control. Release 153 (2011) 198–205, 10.1016/j.jconrel.2011.06.001. [PubMed: 21663778]

[3]. Hanahan D, Robert A Weinberg, Hallmarks of cancer: the next generation, Cell 144 (2011) 646–674, 10.1016/j.cell.2011.02.013. [PubMed: 21376230]

[4]. Allen TM, Cullis PR, Drug delivery systems: entering the mainstream, Science 303 (2004) 1818, 10.1126/science.1095833. [PubMed: 15031496]

[5]. Peer D, Karp JM, Hong S, Farokhzad OC, Margalit R, Langer R, Nanocarriers as an emerging platform for cancer therapy, Nat. Nanotechnol. 2 (2007) 751–760, 10.1038/nnano.2007.387. [PubMed: 18654426]

[6]. Davis ME, Chen Z, Shin DM, Nanoparticle therapeutics: an emerging treatment modality for cancer, Nat. Rev. Drug Discov. 7 (2008) 771–782, 10.1038/nrd2614. [PubMed: 18758474]

[7]. Shi J, Kantoff PW, Wooster R, Farokhzad OC, Cancer nanomedicine: progress, challenges and opportunities, Nat. Rev. Cancer 17 (2016) 20, 10.1038/nrc.2016.108. [PubMed: 27834398]

[8]. Venturoli D, Rippe B, Ficoll and dextran vs. globular proteins as probes for testing glomerular permselectivity: effects of molecular size, shape, charge, and deformability, Am. J. Physiol. Renal Physiol. 288 (2005) F605–F613, 10.1152/ajprenal.00171.2004. [PubMed: 15753324]

[9]. Soo Choi H., Liu W, Misra P, Tanaka E, Zimmer JP, Itty Ipe B, Bawendi MG, Frangioni JV, Renal clearance of quantum dots, Nat. Biotechnol. 25 (2007) 1165–1170, 10.1038/nbt1340. [PubMed: 17891134]

Author Manuscript Author Manuscript Author Manuscript Author Manuscript

[10]. Sarin H, Physiologic upper limits of pore size of different blood capillary types and another perspective on the dual pore theory of microvascular permeability, J. Angiogenes. Res. 2 (2010) 14, 10.1186/2040-2384-2-14. [PubMed: 20701757]

[11]. Iyer AK, Khaled G, Fang J, Maeda H, Exploiting the enhanced permeability and retention effect for tumor targeting, Drug Discov. Today 11 (2006) 812–818, 10.1016/j.drudis.2006.07.005. [PubMed: 16935749]

[12]. Papahadjopoulos D, Allen TM, Gabizon A, Mayhew E, Matthay K, Huang SK, Lee KD, Woodle MC, Lasic DD, Redemann C, Sterically stabilized liposomes: improvements in pharmacokinetics and antitumor therapeutic efficacy, Proc. Natl. Acad. Sci. 88 (1991) 11460, 10.1073/pnas.88.24.11460. [PubMed: 1763060]

[13]. Torchilin VP, Recent advances with liposomes as pharmaceutical carriers, Nat. Rev. Drug Discov. 4 (2005) 145–160, 10.1038/nrd1632. [PubMed: 15688077]

[14]. Petersen GH, Alzghari SK, Chee W, Sankari SS, La-Beck NM, Meta-analysis of clinical and preclinical studies comparing the anticancer efficacy of liposomal versus conventional non-liposomal doxorubicin, J. Control. Release 232 (2016) 255–264, 10.1016/j.jconrel.2016.04.028. [PubMed: 27108612]

[15]. Bourzac K, News feature: cancer nanomedicine, reengineered, Proc. Natl. Acad. Sci. 113 (2016) 12600–12603, 10.1073/pnas.1616895113. [PubMed: 30142085]

[16]. Wilhelm S, Tavares AJ, Chan WCW, Reply to “evaluation of nanomedicines: stick to the basics”, Nat. Rev. Mater. 1 (2016) 16074, 10.1038/natrevmats.2016.74.

[17]. Chan WCW, Nanomedicine 2.0, Acc. Chem. Res. 50 (2017) 627–632, 10.1021/acs.accounts.6b00629. [PubMed: 28945418]

[18]. Wilhelm S, Tavares AJ, Dai Q, Ohta S, Audet J, Dvorak HF, Chan WCW, Analysis of nanoparticle delivery to tumours, Nat. Rev. Mater. 1 (2016) 16014, 10.1038/natrevmats.2016.14.

[19]. Torrice M, Does nanomedicine have a delivery problem? ACS Cent. Sci. 2 (2016) 434–437, 10.1021/acscentsci.6b00190. [PubMed: 27504489]

[20]. Targeting for delivery, Nat. Biomed. Eng. 3 (2019) 671–672, 10.1038/s41551-019-0457-5. [PubMed: 31501568]

[21]. Jain RK, Stylianopoulos T, Delivering nanomedicine to solid tumors, Nat. Rev. Clin. Oncol. 7 (2010) 653, 10.1038/nrclinonc.2010.139. [PubMed: 20838415]

[22]. Blanco E, Shen H, Ferrari M, Principles of nanoparticle design for overcoming biological barriers to drug delivery, Nat. Biotechnol. 33 (2015) 941, 10.1038/nbt.3330. [PubMed: 26348965]

[23]. Zhang Y-R, Lin R, Li H-J, He W.-l., Du J-Z, Wang J, Strategies to improve tumor penetration of nanomedicines through nanoparticle design, Wiley Interdisc. Rev. 11 (2019) e1519,, 10.1002/wnan.1519.

[24]. Pelaz B, Alexiou C, Alvarez-Puebla RA, Alves F, Andrews AM, Ashraf S, Balogh LP, Ballerini L, Bestetti A, Brendel C, Bosi S, Carril M, Chan WCW, Chen C, Chen X, Cheng Z, Cui D, Du J, Dullin C, Escudero A, Feliu N, Gao M, George M, Gogotsi Y, Grünweller A, Gu Z, Halas NJ, Hampp N, Hartmann RK, Hersam MC, Hunziker P, Jian J, Jiang X, Jungebluth P, Kadhiresan P, Kataoka K, Khademhosseini A, Kopeček J, Kotov NA, Krug HF, Lee DS, Lehr C-M, Leong KW, Liang X-J, Ling Lim M, Liz-Marzán LM, Ma X, Macchiarini P, Meng H, Möhwald H, Mulvaney P, Nel AE, Nie S, Nordlander P, Okano T, Oliveira J, Park TH, Penner RM, Prato M, Puntes V, Rotello VM, Samarakoon A, Schaak RE, Shen Y, Sjöqvist S, Skirtach AG, Soliman MG, Stevens MM, Sung H-W, Tang BZ, Tietze R, Udugama BN, VanEpps JS, Weil T, Weiss PS, Willner I, Wu Y, Yang L, Yue Z, Zhang Q, Zhang Q, Zhang X-E, Zhao Y, Zhou X, Parak WJ, Diverse applications of nanomedicine, ACS Nano 11 (2017) 2313–2381, 10.1021/acsnano.6b06040. [PubMed: 28290206]

[25]. Sun Q, Zhou Z, Qiu N, Shen Y, Rational design of cancer nanomedicine: nanoproperty integration and synchronization, Adv. Mater. 29 (2017), 10.1002/adma.201606628.

[26]. Rosenblum D, Joshi N, Tao W, Karp JM, Peer D, Progress and challenges towards targeted delivery of cancer therapeutics, Nat. Commun. 9 (2018) 1410, 10.1038/s41467-018-03705-y. [PubMed: 29650952]

[27]. Yu M, Zheng J, Clearance pathways and tumor targeting of imaging nanoparticles, ACS Nano 9 (2015) 6655–6674, 10.1021/acsnano.5b01320. [PubMed: 26149184]

Author Manuscript Author Manuscript Author Manuscript Author Manuscript

[28]. Zhang Y-N, Poon W, Tavares AJ, McGilvray ID, Chan WCW, Nanoparticle–liver interactions: cellular uptake and hepatobiliary elimination, J. Control. Release 240 (2016) 332–348, 10.1016/j.jconrel.2016.01.020. [PubMed: 26774224]

[29]. Poon W, Zhang Y-N, Ouyang B, Kingston BR, Wu JLY, Wilhelm S, Chan WCW, Elimination pathways of nanoparticles, ACS Nano 13 (2019) 5785–5798, 10.1021/acsnano.9b01383. [PubMed: 30990673]

[30]. von Roemeling C, Jiang W, Chan CK, Weissman IL, Kim BYS, Breaking down the barriers to precision cancer nanomedicine, Trends Biotechnol. 35 (2017) 159–171, 10.1016/j.tibtech.2016.07.006. [PubMed: 27492049]

[31]. Owens DE, Peppas NA, Opsonization, biodistribution, and pharmacokinetics of polymeric nanoparticles, Int. J. Pharm. 307 (2006) 93–102, 10.1016/j.ijpharm.2005.10.010. [PubMed: 16303268]

[32]. Lynch I, Dawson KA, Protein-nanoparticle interactions, Nano Today 3 (2008) 40–47, 10.1016/S1748-0132(08)70014-8.

[33]. Walkey CD, Chan WCW, Understanding and controlling the interaction of nanomaterials with proteins in a physiological environment, Chem. Soc. Rev. 41 (2012) 2780–2799, 10.1039/C1CS15233E. [PubMed: 22086677]

[34]. Tsoi KM, MacParland SA, Ma X-Z, Spetzler VN, Echeverri J, Ouyang B, Fadel SM, Sykes EA, Goldaracena N, Kaths JM, Conneely JB, Alman BA, Selzner M, Ostrowski MA, Adeyi OA, Zilman A, McGilvray ID, Chan WCW, Mechanism of hard-nanomaterial clearance by the liver, Nat. Mater. 15 (2016) 1212, 10.1038/nmat4718. [PubMed: 27525571]

[35]. Tenzer S, Docter D, Kuharev J, Musyanovych A, Fetz V, Hecht R, Schlenk F, Fischer D, Kiouptsi K, Reinhardt C, Landfester K, Schild H, Maskos M, Knauer SK, Stauber RH, Rapid formation of plasma protein corona critically affects nanoparticle pathophysiology, Nat. Nanotechnol. 8 (2013) 772, 10.1038/nnano.2013.181. [PubMed: 24056901]

[36]. Monopoli MP, Åberg C, Salvati A, Dawson KA, Biomolecular coronas provide the biological identity of nanosized materials, Nat. Nanotechnol. 7 (2012) 779, 10.1038/nnano.2012.207. [PubMed: 23212421]

[37]. Salvati A, Pitek AS, Monopoli MP, Prapainop K, Bombelli FB, Hristov DR, Kelly PM, Åberg C, Mahon E, Dawson KA, Transferrin-functionalized nanoparticles lose their targeting capabilities when a biomolecule corona adsorbs on the surface, Nat. Nanotechnol. 8 (2013) 137, 10.1038/nnano.2012.237. [PubMed: 23334168]

[38]. Harris JM, Chess RB, Effect of pegylation on pharmaceuticals, Nat. Rev. Drug Discov. 2 (2003) 214–221, 10.1038/nrd1033. [PubMed: 12612647]

[39]. Jokerst JV, Lobovkina T, Zare RN, Gambhir SS, Nanoparticle PEGylation for imaging and therapy, Nanomedicine 6 (2011) 715–728, 10.2217/nnm.11.19. [PubMed: 21718180]

[40]. Walkey CD, Olsen JB, Guo H, Emili A, Chan WCW, Nanoparticle size and surface chemistry determine serum protein adsorption and macrophage uptake, J. Am. Chem. Soc. 134 (2012) 2139–2147, 10.1021/ja2084338. [PubMed: 22191645]

[41]. Barenholz Y, Doxil® — the first FDA-approved nano-drug: lessons learned, J. Control. Release 160 (2012) 117–134, 10.1016/j.jconrel.2012.03.020. [PubMed: 22484195]

[42]. He Q, Zhang Z, Gao F, Li Y, Shi J, In vivo biodistribution and urinary excretion of mesoporous silica nanoparticles: effects of particle size and PEGylation, Small 7 (2011) 271–280, 10.1002/smll.201001459. [PubMed: 21213393]

[43]. Dai Q, Walkey C, Chan WCW, Polyethylene glycol backfilling mitigates the negative impact of the protein corona on nanoparticle cell targeting, Angew. Chem. Int. Ed. 53 (2014) 5093–5096, 10.1002/anie.201309464.

[44]. Gref R, Lück M, Quellec P, Marchand M, Dellacherie E, Harnisch S, Blunk T, Müller RH, ‘Stealth’ corona-core nanoparticles surface modified by polyethylene glycol (PEG): influences of the corona (PEG chain length and surface density) and of the core composition on phagocytic uptake and plasma protein adsorption, Colloids Surf. B: Biointerfaces 18 (2000) 301–313, 10.1016/S0927-7765(99)00156-3. [PubMed: 10915952]

[45]. Mori A, Klibanov AL, Torchilin VP, Huang L, Influence of the steric barrier activity of amphipathic poly(ethyleneglycol) and ganglioside GM1 on the circulation time of liposomes

Author Manuscript Author Manuscript Author Manuscript Author Manuscript

and on the target binding of immunoliposomes in vivo, FEBS Lett. 284 (1991) 263–266, 10.1016/0014-5793(91)80699-4. [PubMed: 2060647]

[46]. Daou TJ, Li L, Reiss P, Josserand V, Texier I, Effect of poly(ethylene glycol) length on the in vivo behavior of coated quantum dots, Langmuir 25 (2009) 3040–3044, 10.1021/la8035083. [PubMed: 19437711]

[47]. Perrault SD, Walkey C, Jennings T, Fischer HC, Chan WCW, Mediating tumor targeting efficiency of nanoparticles through design, Nano Lett. 9 (2009) 1909–1915, 10.1021/nl900031y. [PubMed: 19344179]

[48]. Bertrand N, Grenier P, Mahmoudi M, Lima EM, Appel EA, Dormont F, Lim J-M, Karnik R, Langer R, Farokhzad OC, Mechanistic understanding of in vivo protein corona formation on polymeric nanoparticles and impact on pharmacokinetics, Nat. Commun. 8 (2017) 777, 10.1038/s41467-017-00600-w. [PubMed: 28974673]

[49]. Ladd J, Zhang Z, Chen S, Hower JC, Jiang S, Zwitterionic polymers exhibiting high resistance to nonspecific protein adsorption from human serum and plasma, Biomacromolecules 9 (2008) 1357–1361, 10.1021/bm701301s. [PubMed: 18376858]

[50]. Jiang S, Cao Z, Ultralow-fouling, functionalizable, and hydrolyzable zwitterionic materials and their derivatives for biological applications, Adv. Mater. 22 (2010) 920–932, 10.1002/adma.200901407. [PubMed: 20217815]

[51]. Liu J, Yu M, Ning X, Zhou C, Yang S, Zheng J, PEGylation and zwitterionization: pros and cons in the renal clearance and tumor targeting of near-IR-emitting gold nanoparticles, Angew. Chem. Int. Ed. 52 (2013) 12572–12576, 10.1002/anie.201304465.

[52]. García KP, Zarschler K, Barbaro L, Barreto JA, O'Malley W, Spiccia L, Stephan H, Graham B, Zwitterionic-coated "stealth" nanoparticles for biomedical applications: recent advances in countering biomolecular corona formation and uptake by the mononuclear phagocyte system, Small 10 (2014) 2516–2529, 10.1002/smll.201303540. [PubMed: 24687857]

[53]. Kang H, Gravier J, Bao K, Wada H, Lee JH, Baek Y, El Fakhri G, Gioux S, Rubin BP, Coll J-L, Choi HS, Renal clearable organic nanocarriers for bioimaging and drug delivery, Adv. Mater. 28 (2016) 8162–8168, 10.1002/adma.201601101. [PubMed: 27414255]

[54]. Hu C-MJ, Zhang L, Aryal S, Cheung C, Fang RH, Zhang L, Erythrocyte membrane-camouflaged polymeric nanoparticles as a biomimetic delivery platform, Proc. Natl. Acad. Sci. 108 (2011) 10980, 10.1073/pnas.1106634108. [PubMed: 21690347]

[55]. Hu C-MJ, Fang RH, Wang K-C, Luk BT, Thamphiwatana S, Dehaini D, Nguyen P, Angsantikul P, Wen CH, Kroll AV, Carpenter C, Ramesh M, Qu V, Patel SH, Zhu J, Shi W, Hofman FM, Chen TC, Gao W, Zhang K, Chien S, Zhang L, Nanoparticle biointerfacing by platelet membrane cloaking, Nature 526 (2015) 118, 10.1038/nature15373. [PubMed: 26374997]

[56]. Hu Q, Sun W, Qian C, Wang C, Bomba HN, Gu Z, Anticancer platelet-mimicking nanovehicles, Adv. Mater. 27 (2015) 7043–7050, 10.1002/adma.201503323. [PubMed: 26416431]

[57]. Fang RH, Jiang Y, Fang JC, Zhang L, Cell membrane-derived nanomaterials for biomedical applications, Biomaterials 128 (2017) 69–83, 10.1016/j.biomaterials.2017.02.041. [PubMed: 28292726]

[58]. Rodriguez PL, Harada T, Christian DA, Pantano DA, Tsai RK, Discher DE, Minimal "self" peptides that inhibit phagocytic clearance and enhance delivery of nanoparticles, Science 339 (2013) 971–975, 10.1126/science.1229568. [PubMed: 23430657]

[59]. Tavares AJ, Poon W, Zhang Y-N, Dai Q, Besla R, Ding D, Ouyang B, Li A, Chen J, Zheng G, Robbins C, Chan WCW, Effect of removing Kupffer cells on nanoparticle tumor delivery, Proc. Natl. Acad. Sci. 114 (2017) E10871–E10880, 10.1073/pnas.1713390114. [PubMed: 29208719]

[60]. Folkman J, Tumor angiogenesis: therapeutic implications, N. Engl. J. Med. 285 (1971) 1182–1186, 10.1056/nejm197111182852108. [PubMed: 4938153]

[61]. Dvorak HF, Brown LF, Detmar M, Dvorak AM, Vascular permeability factor/vascular endothelial growth factor, microvascular hyperpermeability, and angiogenesis, Am. J. Pathol. 146 (1995) 1029–1039. [PubMed: 7538264]

[62]. Carmeliet P, Jain RK, Angiogenesis in cancer and other diseases, Nature 407 (2000) 249–257, 10.1038/35025220. [PubMed: 11001068]

[63]. Baish JW, Jain RK, Fractals and cancer, Cancer Res. 60 (2000) 3683–3688. [PubMed: 10919633]

Author Manuscript Author Manuscript Author Manuscript Author Manuscript

[64]. Conway EM, Collen D, Carmeliet P, Molecular mechanisms of blood vessel growth, Cardiovasc. Res. 49 (2001) 507–521, 10.1016/s0008-6363(00)00281-9. [PubMed: 11166264]

[65]. Jain RK, Transport of molecules across tumor vasculature, Cancer Metastasis Rev. 6 (1987) 559–593, 10.1007/BF00047468. [PubMed: 3327633]

[66]. Sevick EM, Jain RK, Geometric resistance to blood flow in solid tumors perfused < em >ex vivo: < /em > effects of tumor size and perfusion pressure, Cancer Res. 49 (1989) 3506–3512. [PubMed: 2731172]

[67]. Heldin C-H, Rubin K, Pietras K, Östman A, High interstitial fluid pressure — an obstacle in cancer therapy, Nat. Rev. Cancer 4 (2004) 806–813, 10.1038/nrc1456. [PubMed: 15510161]

[68]. Jain RK, Tong RT, Munn LL, Effect of vascular normalization by antiangiogenic therapy on interstitial hypertension, peritumor edema, and lymphatic metastasis: insights from a mathematical model, Cancer Res. 67 (2007) 2729–2735, 10.1158/0008-5472.can-06-4102. [PubMed: 17363594]

[69]. Boucher Y, Baxter LT, Jain RK, Interstitial pressure gradients in tissue-isolated and subcutaneous tumors: implications for therapy, Cancer Res. 50 (1990) 4478–4484. [PubMed: 2369726]

[70]. DiResta GR, Lee J, Larson SM, Arbit E, Characterization of neuroblastoma xenograft in rat flank. I. Growth, interstitial fluid pressure, and interstitial fluid velocity distribution profiles, Microvasc. Res. 46 (1993) 158–177, 10.1006/mvre.1993.1044. [PubMed: 8246816]

[71]. Boucher Y, Jain RK, Microvascular pressure is the principal driving force for interstitial hypertension in solid tumors: implications for vascular collapse, Cancer Res. 52 (1992) 5110–5114. [PubMed: 1516068]

[72]. Netti PA, Roberge S, Boucher Y, Baxter LT, Jain RK, Effect of transvascular fluid exchange on pressure–flow relationship in tumors: a proposed mechanism for tumor blood flow heterogeneity, Microvasc. Res. 52 (1996) 27–46, 10.1006/mvre.1996.0041. [PubMed: 8812751]

[73]. Baish JW, Netti PA, Jain RK, Transmural coupling of fluid flow in microcirculatory network and interstitium in tumors, Microvasc. Res. 53 (1997) 128–141, 10.1006/mvre.1996.2005. [PubMed: 9143544]

[74]. Jain RK, Transport of molecules in the tumor interstitium: a review, Cancer Res. 47 (1987) 3039–3051. [PubMed: 3555767]

[75]. Yuan F, Leunig M, Huang SK, Berk DA, Papahadjopoulos D, Jain RK, Mirovascular permeability and interstitial penetration of sterically stabilized (stealth) liposomes in a human tumor xenograft, Cancer Res. 54 (1994) 3352–3356. [PubMed: 8012948]

[76]. Chauhan VP, Popović Z, Chen O, Cui J, Fukumura D, Bawendi MG, Jain RK, Fluorescent nanorods and nanospheres for real-time in vivo probing of nanoparticle shape-dependent tumor penetration, Angew. Chem. Int. Ed. 50 (2011) 11417–11420, 10.1002/anie.201104449.

[77]. Smith BR, Kempen P, Bouley D, Xu A, Liu Z, Melosh N, Dai H, Sinclair R, Gambhir SS, Shape matters: intravital microscopy reveals surprising geometrical dependence for nanoparticles in tumor models of extravasation, Nano Lett. 12 (2012) 3369–3377, 10.1021/nl204175t. [PubMed: 22650417]

[78]. Liang Q, Bie N, Yong T, Tang K, Shi X, Wei Z, Jia H, Zhang X, Zhao H, Huang W, Gan L, Huang B, Yang X, The softness of tumour-cell-derived microparticles regulates their drug-delivery efficiency, Nat. Biomed. Eng. 3 (2019) 729–740, 10.1038/s41551-019-0405-4. [PubMed: 31110292]

[79]. Zhou Q, Shao S, Wang J, Xu C, Xiang J, Piao Y, Zhou Z, Yu Q, Tang J, Liu X, Gan Z, Mo R, Gu Z, Shen Y, Enzyme-activatable polymer–drug conjugate augments tumour penetration and treatment efficacy, Nat. Nanotechnol. 14 (2019) 799–809, 10.1038/s41565-019-0485-z. [PubMed: 31263194]

[80]. Sugahara KN, Teesalu T, Karmali PP, Kotamraju VR, Agemy L, Greenwald DR, Ruoslahti E, Coadministration of a tumor-penetrating peptide enhances the efficacy of cancer drugs, Science 328 (2010) 1031–1035, 10.1126/science.1183057. [PubMed: 20378772]

[81]. Liu X, Lin P, Perrett I, Lin J, Liao Y-P, Chang CH, Jiang J, Wu N, Donahue T, Wainberg Z, Nel AE, Meng H, Tumor-penetrating peptide enhances transcytosis of silicasome-based chemotherapy for pancreatic cancer, J. Clin. Invest. 127 (2017) 2007–2018, 10.1172/JCI92284. [PubMed: 28414297]

Author Manuscript Author Manuscript Author Manuscript Author Manuscript

[82]. Roger E, Lagarce F, Garcion E, Benoit JP, Lipid nanocarriers improve paclitaxel transport throughout human intestinal epithelial cells by using vesicle-mediated transcytosis, J. Control. Release 140 (2009) 174–181, 10.1016/j.jconrel.2009.08.010. [PubMed: 19699246]

[83]. Miura S, Suzuki H, Bae YH, A multilayered cell culture model for transport study in solid tumors: evaluation of tissue penetration of polyethyleneimine based cationic micelles, Nano Today 9 (2014) 695–704, 10.1016/j.nantod.2014.10.003. [PubMed: 25866552]

[84]. Sugahara KN, Teesalu T, Karmali PP, Kotamraju VR, Agemy L, Girard OM, Hanahan D, Mattrey RF, Ruoslahti E, Tissue-penetrating delivery of compounds and nanoparticles into tumors, Cancer Cell 16 (2009) 510–520, 10.1016/j.ccr.2009.10.013. [PubMed: 19962669]

[85]. Chauhan VP, Stylianopoulos T, Martin JD, Popović Z, Chen O, Kamoun WS, Bawendi MG, Fukumura D, Jain RK, Normalization of tumour blood vessels improves the delivery of nanomedicines in a size-dependent manner, Nat. Nanotechnol. 7 (2012) 383, 10.1038/nnano.2012.45. [PubMed: 22484912]

[86]. Jain RK, Normalization of tumor vasculature: an emerging concept in antiangiogenic therapy, Science 307 (2005) 58–62, 10.1126/science.1104819. [PubMed: 15637262]

[87]. Fukumura D, Kloepper J, Amoozgar Z, Duda DG, Jain RK, Enhancing cancer immunotherapy using antiangiogenics: opportunities and challenges, Nat. Rev. Clin. Oncol. 15 (2018) 325–340, 10.1038/nrclinonc.2018.29. [PubMed: 29508855]

[88]. Yancopoulos GD, Davis S, Gale NW, Rudge JS, Wiegand SJ, Holash J, Vascular-specific growth factors and blood vessel formation, Nature 407 (2000) 242–248, 10.1038/35025215. [PubMed: 11001067]

[89]. Willett CG, Boucher Y, di Tomaso E, Duda DG, Munn LL, Tong RT, Chung DC, Sahani DV, Kalva SP, Kozin SV, Mino M, Cohen KS, Scadden DT, Hartford AC, Fischman AJ, Clark JW, Ryan DP, Zhu AX, Blaszkowsky LS, Chen HX, Shellito PC, Lauwers GY, Jain RK, Direct evidence that the VEGF-specific antibody bevacizumab has antivascular effects in human rectal cancer, Nat. Med. 10 (2004) 145–147, 10.1038/nm988. [PubMed: 14745444]

[90]. Jain RK, Duda DG, Clark JW, Loeffler JS, Lessons from phase III clinical trials on anti-VEGF therapy for cancer, Nat. Clin. Pract. Oncol. 3 (2006) 24–40, 10.1038/ncponc0403. [PubMed: 16407877]

[91]. Monsky WL, Fukumura D, Gohongi T, Ancukiewcz M, Weich HA, Torchilin VP, Yuan F, Jain RK, Augmentation of transvascular transport of macromolecules and nanoparticles in tumors using vascular endothelial growth factor, Cancer Res. 59 (1999) 4129–4135. [PubMed: 10463618]

[92]. Hernot S, Klibanov AL, Microbubbles in ultrasound-triggered drug and gene delivery, Adv. Drug Deliv. Rev. 60 (2008) 1153–1166, 10.1016/j.addr.2008.03.005. [PubMed: 18486268]

[93]. Qiu Y, Tong S, Zhang L, Sakurai Y, Myers DR, Hong L, Lam WA, Bao G, Magnetic forces enable controlled drug delivery by disrupting endothelial cell-cell junctions, Nat. Commun. 8 (2017) 15594, 10.1038/ncomms15594. [PubMed: 28593939]

[94]. Frazier N, Ghandehari H, Hyperthermia approaches for enhanced delivery of nanomedicines to solid tumors, Biotechnol. Bioeng. 112 (2015) 1967–1983, 10.1002/bit.25653. [PubMed: 25995079]

[95]. Netti PA, Berk DA, Swartz MA, Grodzinsky AJ, Jain RK, Role of extracellular matrix assembly in interstitial transport in solid tumors, Cancer Res. 60 (2000) 2497–2503. [PubMed: 10811131]

[96]. Lu P, Weaver VM, Werb Z, The extracellular matrix: a dynamic niche in cancer progression, J. Cell Biol. 196 (2012) 395–406, 10.1083/jcb.201102147. [PubMed: 22351925]

[97]. Cabral H, Matsumoto Y, Mizuno K, Chen Q, Murakami M, Kimura M, Terada Y, Kano MR, Miyazono K, Uesaka M, Nishiyama N, Kataoka K, Accumulation of sub-100 nm polymeric micelles in poorly permeable tumours depends on size, Nat. Nanotechnol. 6 (2011) 815–823, 10.1038/nnano.2011.166. [PubMed: 22020122]

[98]. Miller MA, Zheng Y-R, Gadde S, Pfirschke C, Zope H, Engblom C, Kohler RH, Iwamoto Y, Yang KS, Askevold B, Kolishetti N, Pittet M, Lippard SJ, Farokhzad OC, Weissleder R, Tumour-associated macrophages act as a slow-release reservoir of nano-therapeutic Pt(IV) pro-drug, Nat. Commun. 6 (2015) 8692, 10.1038/ncomms9692. [PubMed: 26503691]

Author Manuscript Author Manuscript Author Manuscript Author Manuscript

[99]. Dai Q, Wilhelm S, Ding D, Syed AM, Sindhwani S, Zhang Y, Chen YY, MacMillan P, Chan WCW, Quantifying the ligand-coated nanoparticle delivery to cancer cells in solid tumors, ACS Nano 12 (2018) 8423–8435, 10.1021/acsnano.8b03900. [PubMed: 30016073]

[100]. Höckel M, Vaupel P, Biological consequences of tumor hypoxia, Semin. Oncol. 28 (2001) 36–41, 10.1016/S0093-7754(01)90211-8.

[101]. Wilson WR, Hay MP, Targeting hypoxia in cancer therapy, Nat. Rev. Cancer 11 (2011) 393–410, 10.1038/nrc3064. [PubMed: 21606941]

[102]. Rohwer N, Cramer T, Hypoxia-mediated drug resistance: novel insights on the functional interaction of HIFs and cell death pathways, Drug Resist. Updat. 14 (2011) 191–201, 10.1016/j.drup.2011.03.001. [PubMed: 21466972]

[103]. Li X, Kwon N, Guo T, Liu Z, Yoon J, Innovative strategies for hypoxic-tumor photodynamic therapy, Angew. Chem. Int. Ed. 57 (2018) 11522–11531, 10.1002/anie.201805138.

[104]. Donahue ND, Acar H, Wilhelm S, Concepts of nanoparticle cellular uptake, intracellular trafficking, and kinetics in nanomedicine, Adv. Drug Deliv. Rev. 143 (2019) 68–96, 10.1016/j.addr.2019.04.008. [PubMed: 31022434]

[105]. Liu Y, Huo Y, Yao L, Xu Y, Meng F, Li H, Sun K, Zhou G, Kohane DS, Tao K, Transcytosis of nanomedicine for tumor penetration, Nano Lett. 19 (2019) 8010–8020, 10.1021/acs.nanolett.9b03211. [PubMed: 31639306]

[106]. Mura S, Nicolas J, Couvreur P, Stimuli-responsive nanocarriers for drug delivery, Nat. Mater. 12 (2013) 991–1003, 10.1038/nmat3776. [PubMed: 24150417]

[107]. Lu Y, Aimetti AA, Langer R, Gu Z, Bioresponsive materials, Nat. Rev. Mater. 2 (2016) 16075, 10.1038/natrevmats.2016.75.

[108]. Zhou Z, Shen Y, Tang J, Fan M, Van Kirk E.A., Murdoch WJ, Radosz M, Charge-reversal drug conjugate for targeted cancer cell nuclear drug delivery, Adv. Funct. Mater. 19 (2009) 3580–3589, 10.1002/adfm.200900825.

[109]. Yuan Y-Y, Mao C-Q, Du X-J, Du J-Z, Wang F, Wang J, Surface charge switchable nanoparticles based on zwitterionic polymer for enhanced drug delivery to tumor, Adv. Mater. 24 (2012) 5476–5480, 10.1002/adma.201202296. [PubMed: 22886872]

[110]. Li H-J, Du J-Z, Du X-J, Xu C-F, Sun C-Y, Wang H-X, Cao Z-T, Yang X-Z, Zhu Y-H, Nie S, Wang J, Stimuli-responsive clustered nanoparticles for improved tumor penetration and therapeutic efficacy, Proc. Natl. Acad. Sci. 113 (2016) 4164–4169, 10.1073/pnas.1522080113. [PubMed: 27035960]

[111]. Feng Q, Wilhelm J, Gao J, Transistor-like ultra-pH-sensitive polymeric nanoparticles, Acc. Chem. Res. 52 (2019) 1485–1495, 10.1021/acs.accounts.9b00080. [PubMed: 31067025]

[112]. Brown E, McKee T, di Tomaso E, Pluen A, Seed B, Boucher Y, Jain RK, Dynamic imaging of collagen and its modulation in tumors in vivo using second-harmonic generation, Nat. Med. 9 (2003) 796–800, 10.1038/nm879. [PubMed: 12754503]

[113]. Mok W, Boucher Y, Jain RK, Matrix metalloproteinases-1 and −8 improve the distribution and efficacy of an oncolytic virus, Cancer Res. 67 (2007) 10664–10668, 10.1158/0008-5472.can-07-3107. [PubMed: 18006807]

[114]. Kim J-H, Lee Y-S, Kim H, Huang J-H, Yoon A-R, Yun C-O, Relaxin expression from tumor-targeting adenoviruses and its intratumoral spread, apoptosis induction, and efficacy, J. Nat. Cancer Inst. 98 (2006) 1482–1493, 10.1093/jnci/djj397. [PubMed: 17047197]

[115]. Neeves KB, Sawyer AJ, Foley CP, Saltzman WM, Olbricht WL, Dilation and degradation of the brain extracellular matrix enhances penetration of infused polymer nanoparticles, Brain Res. 1180 (2007) 121–132, 10.1016/j.brainres.2007.08.050. [PubMed: 17920047]

[116]. Goodman TT, Olive PL, Pun SH, Increased nanoparticle penetration in collagenase-treated multicellular spheroids, Int. J. Nanomedicine 2 (2007) 265–274. [PubMed: 17722554]

[117]. Diop-Frimpong B, Chauhan VP, Krane S, Boucher Y, Jain RK, Losartan inhibits collagen I synthesis and improves the distribution and efficacy of nanotherapeutics in tumors, Proc. Natl. Acad. Sci. 108 (2011) 2909–2914, 10.1073/pnas.1018892108. [PubMed: 21282607]

[118]. Miao L, Newby JM, Lin CM, Zhang L, Xu F, Kim WY, Forest MG, Lai SK, Milowsky MI, Wobker SE, Huang L, The binding site barrier elicited by tumor-associated fibroblasts interferes

Author Manuscript Author Manuscript Author Manuscript Author Manuscript

disposition of nanoparticles in stroma-vessel type tumors, ACS Nano 10 (2016) 9243–9258, 10.1021/acsnano.6b02776. [PubMed: 27666558]

[119]. Peng C, Yu M, Hsieh J-T, Kapur P, Zheng J, Correlating anticancer drug delivery efficiency with vascular permeability of renal clearable versus non-renal clearable nanocarriers, Angew. Chem. Int. Ed. 58 (2019) 12076–12080, 10.1002/anie.201905738.

[120]. Jiang W, Kim BYS, Rutka JT, Chan WCW, Nanoparticle-mediated cellular response is size-dependent, Nat. Nanotechnol. 3 (2008) 145–150, 10.1038/nnano.2008.30. [PubMed: 18654486]

[121]. Verma A, Stellacci F, Effect of surface properties on nanoparticle–cell interactions, Small 6 (2010) 12–21, 10.1002/smll.200901158. [PubMed: 19844908]

[122]. Zeisberger SM, Odermatt B, Marty C, Zehnder-Fjällman AHM, Ballmer-Hofer K, Schwendener RA, Clodronate-liposome-mediated depletion of tumour-associated macrophages: a new and highly effective antiangiogenic therapy approach, Br. J. Cancer 95 (2006) 272–281, 10.1038/sj.bjc.6603240. [PubMed: 16832418]

[123]. Opperman KS, Vandyke K, Clark KC, Coulter EA, Hewett DR, Mrozik KM, Schwarz N, Evdokiou A, Croucher PI, Psaltis PJ, Noll JE, Zannettino ACW, Clodronate-liposome mediated macrophage depletion abrogates multiple myeloma tumor establishment in vivo, Neoplasia 21 (2019) 777–787, 10.1016/j.neo.2019.05.006. [PubMed: 31247457]

[124]. Zhang W, Zhu X-D, Sun H-C, Xiong Y-Q, Zhuang P-Y, Xu H-X, Kong L-Q, Wang L, Wu W-Z, Tang Z-Y, Depletion of tumor-associated macrophages enhances the effect of sorafenib in metastatic liver cancer models by antimetastatic and antiangiogenic effects, Clin. Cancer Res. 16 (2010) 3420–3430, 10.1158/1078-0432.ccr-09-2904. [PubMed: 20570927]

[125]. Olive KP, Jacobetz MA, Davidson CJ, Gopinathan A, McIntyre D, Honess D, Madhu B, Goldgraben MA, Caldwell ME, Allard D, Frese KK, DeNicola G, Feig C, Combs C, Winter SP, Ireland-Zecchini H, Reichelt S, Howat WJ, Chang A, Dhara M, Wang L, Rückert F, Grützmann R, Pilarsky C, Izeradjene K, Hingorani SR, Huang P, Davies SE, Plunkett W, Egorin M, Hruban RH, Whitebread N, McGovern K, Adams J, Iacobuzio-Donahue C, Griffiths J, Tuveson DA, Inhibition of hedgehog signaling enhances delivery of chemotherapy in a mouse model of pancreatic cancer, Science 324 (2009) 1457–1461, 10.1126/science.1171362. [PubMed: 19460966]

[126]. Du B, Yu M, Zheng J, Transport and interactions of nanoparticles in the kidneys, Nat. Rev. Mater. 3 (2018) 358–374, 10.1038/s41578-018-0038-3.

[127]. Burns AA, Vider J, Ow H, Herz E, Penate-Medina O, Baumgart M, Larson SM, Wiesner U, Bradbury M, Fluorescent silica nanoparticles with efficient urinary excretion for nanomedicine, Nano Lett. 9 (2009) 442–448, 10.1021/nl803405h. [PubMed: 19099455]

[128]. Muhammed MAH, Verma PK, Pal SK, Kumar RCA, Paul S, Omkumar RV, Pradeep T, Bright NIR-emitting Au23 from Au25: characterization and applications including biolabeling, Chem. Eur. J. 15 (2009) 10110–10120, 10.1002/chem.200901425. [PubMed: 19711391]

[129]. Ruggiero A, Villa CH, Bander E, Rey DA, Bergkvist M, Batt CA, Manova-Todorova K, Deen WM, Scheinberg DA, McDevitt MR, Paradoxical glomerular filtration of carbon nanotubes, Proc. Natl. Acad. Sci. 107 (2010) 12369, 10.1073/pnas.0913667107. [PubMed: 20566862]

[130]. Zhou C, Long M, Qin Y, Sun X, Zheng J, Luminescent gold nanoparticles with efficient renal clearance, Angew. Chem. Int. Ed. 50 (2011) 3168–3172, 10.1002/anie.201007321.

[131]. Huang X, Zhang F, Zhu L, Choi KY, Guo N, Guo J, Tackett K, Anilkumar P, Liu G, Quan Q, Choi HS, Niu G, Sun Y-P, Lee S, Chen X, Effect of injection routes on the biodistribution, clearance, and tumor uptake of carbon dots, ACS Nano 7 (2013) 5684–5693, 10.1021/nn401911k. [PubMed: 23731122]

[132]. Cao T, Yang Y, Sun Y, Wu Y, Gao Y, Feng W, Li F, Biodistribution of sub-10 nm PEG-modified radioactive/upconversion nanoparticles, Biomaterials 34 (2013) 7127–7134, 10.1016/j.biomaterials.2013.05.028. [PubMed: 23796579]

[133]. Chen H, Wang GD, Tang W, Todd T, Zhen Z, Tsang C, Hekmatyar K, Cowger T, Hubbard RB, Zhang W, Stickney J, Shen B, Xie J, Gd-encapsulated carbonaceous dots with efficient renal clearance for magnetic resonance imaging, Adv. Mater. 26 (2014) 6761–6766, 10.1002/adma.201402964. [PubMed: 25178894]

Author Manuscript Author Manuscript Author Manuscript Author Manuscript

[134]. Tang S, Chen M, Zheng N, Sub-10-nm Pd nanosheets with renal clearance for efficient near-infrared photothermal cancer therapy, Small 10 (2014) 3139–3144, 10.1002/smll.201303631. [PubMed: 24729448]

[135]. Zhao Y, Sultan D, Detering L, Luehmann H, Liu Y, Facile synthesis, pharmacokinetic and systemic clearance evaluation, and positron emission tomography cancer imaging of 64Cu–au alloy nanoclusters, Nanoscale 6 (2014) 13501–13509, 10.1039/C4NR04569F. [PubMed: 25266128]

[136]. Zhou M, Li J, Liang S, Sood AK, Liang D, Li C, CuS nanodots with ultrahigh efficient renal clearance for positron emission tomography imaging and image-guided photothermal therapy, ACS Nano 9 (2015) 7085–7096, 10.1021/acsnano.5b02635. [PubMed: 26098195]

[137]. Cheng L, Jiang D, Kamkaew A, Valdovinos HF, Im H-J, Feng L, England CG, Goel S, Barnhart TE, Liu Z, Cai W, Renal-clearable PEGylated porphyrin nanoparticles for image-guided photodynamic cancer therapy, Adv. Funct. Mater. 27 (2017) 1702928, 10.1002/adfm.201702928. [PubMed: 29151826]

[138]. Shen S, Jiang D, Cheng L, Chao Y, Nie K, Dong Z, Kutyreff CJ, Engle JW, Huang P, Cai W, Liu Z, Renal-clearable ultrasmall coordination polymer nanodots for chelator-free 64Cu-labeling and imaging-guided enhanced radiotherapy of cancer, ACS Nano 11 (2017) 9103–9111, 10.1021/acsnano.7b03857. [PubMed: 28853861]

[139]. Xu J, Peng C, Yu M, Zheng J, Renal clearable noble metal nanoparticles: photoluminescence, elimination, and biomedical applications, Wiley Interdisc. Rev. 9 (2017) e1453,, 10.1002/wnan.1453.

[140]. Tan L, Wan J, Guo W, Ou C, Liu T, Fu C, Zhang Q, Ren X, Liang X-J, Ren J, Li L, Meng X, Renal-clearable quaternary chalcogenide nanocrystal for photoacoustic/magnetic resonance imaging guided tumor photothermal therapy, Biomaterials 159 (2018) 108–118, 10.1016/j.biomaterials.2018.01.003. [PubMed: 29316452]

[141]. Jiang D, Im H-J, Boleyn ME, England CG, Ni D, Kang L, Engle JW, Huang P, Lan X, Cai W, Efficient renal clearance of DNA tetrahedron nanoparticles enables quantitative evaluation of kidney function, Nano Res. 12 (2019) 637–642, 10.1007/s12274-019-2271-5. [PubMed: 32055285]

[142]. Choi HS, Nasr K, Alyabyev S, Feith D, Lee JH, Kim SH, Ashitate Y, Hyun H, Patonay G, Strekowski L, Henary M, Frangioni JV, Synthesis and in vivo fate of zwitterionic near-infrared fluorophores, Angew. Chem. Int. Ed. 50 (2011) 6258–6263, 10.1002/anie.201102459.

[143]. Huang J, Li J, Lyu Y, Miao Q, Pu K, Molecular optical imaging probes for early diagnosis of drug-induced acute kidney injury, Nat. Mater. 18 (2019) 1133–1143, 10.1038/s41563-019-0378-4. [PubMed: 31133729]

[144]. Park J-H, Gu L, von Maltzahn G., Ruoslahti E, Bhatia SN, Sailor MJ, Biodegradable luminescent porous silicon nanoparticles for in vivo applications, Nat. Mater. 8 (2009) 331–336, 10.1038/nmat2398. [PubMed: 19234444]

[145]. Hu X, Sun J, Li F, Li R, Wu J, He J, Wang N, Liu J, Wang S, Zhou F, Sun X, Kim D, Hyeon T, Ling D, Renal-clearable hollow bismuth subcarbonate nanotubes for tumor targeted computed tomography imaging and chemoradiotherapy, Nano Lett. 18 (2018) 1196–1204, 10.1021/acs.nanolett.7b04741. [PubMed: 29297694]

[146]. Wei R, Cai Z, Ren BW, Li A, Lin H, Zhang K, Chen H, Shan H, Ai H, Gao J, Biodegradable and renal-clearable hollow porous iron oxide nanoboxes for in vivo imaging, Chem. Mater. 30 (2018) 7950–7961, 10.1021/acs.chemmater.8b03564.

[147]. Wei Q, Chen Y, Ma X, Ji J, Qiao Y, Zhou B, Ma F, Ling D, Zhang H, Tian M, Tian J, Zhou M, High-efficient clearable nanoparticles for multi-modal imaging and image-guided cancer therapy, Adv. Funct. Mater. 28 (2018), 10.1002/adfm.201704634.

[148]. Lacerda L, Soundararajan A, Singh R, Pastorin G, Al-Jamal KT, Turton J, Frederik P, Herrero MA, Li S, Bao A, Emfietzoglou D, Mather S, Phillips WT, Prato M, Bianco A, Goins B, Kostarelos K, Dynamic imaging of functionalized multi-walled carbon nanotube systemic circulation and urinary excretion, Adv. Mater. 20 (2008) 225–230, 10.1002/adma.200702334.

[149]. Liu J, Yu M, Zhou C, Yang S, Ning X, Zheng J, Passive tumor targeting of renal-clearable luminescent gold nanoparticles: long tumor retention and fast normal tissue clearance, J. Am. Chem. Soc. 135 (2013) 4978–4981, 10.1021/ja401612x. [PubMed: 23506476]

Author Manuscript Author Manuscript Author Manuscript Author Manuscript

[150]. Baish JW, Stylianopoulos T, Lanning RM, Kamoun WS, Fukumura D, Munn LL, Jain RK, Scaling rules for diffusive drug delivery in tumor and normal tissues, Proc. Natl. Acad. Sci. 108 (2011) 1799, 10.1073/pnas.1018154108. [PubMed: 21224417]

[151]. Peng C, Xu J, Yu M, Ning X, Huang Y, Du B, Hernandez E, Kapur P, Hsieh J-T, Zheng J, Tuning the in vivo transport of anticancer drugs using renal-clearable gold nanoparticles, Angew. Chem. Int. Ed. 58 (2019) 8479–8483, 10.1002/anie.201903256.

[152]. Benezra M, Penate-Medina O, Zanzonico PB, Schaer D, Ow H, Burns A, DeStanchina E, Longo V, Herz E, Iyer S, Wolchok J, Larson SM, Wiesner U, Bradbury MS, Multimodal silica nanoparticles are effective cancer-targeted probes in a model of human melanoma, J. Clin. Invest. 121 (2011) 2768–2780, 10.1172/JCI45600. [PubMed: 21670497]

[153]. Xu J, Yu M, Peng C, Carter P, Tian J, Ning X, Zhou Q, Tu Q, Zhang G, Dao A, Jiang X, Kapur P, Hsieh J-T, Zhao X, Liu P, Zheng J, Dose dependencies and biocompatibility of renal clearable gold nanoparticles: from mice to non-human primates, Angew. Chem. Int. Ed. 57 (2018) 266–271, 10.1002/anie.201710584.

[154]. Kang H, Rho S, Stiles WR, Hu S, Baek Y, Hwang DW, Kashiwagi S, Kim MS, Choi HS, Size-dependent EPR effect of polymeric nanoparticles on tumor targeting, Adv. Healthc. Mater. 9 (2020) 1901223, 10.1002/adhm.201901223.

[155]. Du B, Jiang X, Huang Y, Li S, Lin JC, Yu M, Zheng J, Tailoring kidney transport of organic dyes with low-molecular-weight PEGylation, Bioconjug. Chem. (2019), 10.1021/acs.bioconjchem.9b00707.

[156]. Tang S, Peng C, Xu J, Du B, Wang Q, Vinluan Iii R.D., Yu M, Kim MJ, Zheng J, Tailoring renal clearance and tumor targeting of Ultrasmall metal nanoparticles with particle density, Angew. Chem. 128 (2016) 16273–16277, 10.1002/ange.201609043.

[157]. Chen F, Ma K, Benezra M, Zhang L, Cheal SM, Phillips E, Yoo B, Pauliah M, Overholtzer M, Zanzonico P, Sequeira S, Gonen M, Quinn T, Wiesner U, Bradbury MS, Cancer-targeting ultrasmall silica nanoparticles for clinical translation: physicochemical structure and biological property correlations, Chem. Mater. 29 (2017) 8766–8779, 10.1021/acs.chemmater.7b03033. [PubMed: 29129959]

[158]. Chen F, Ma K, Zhang L, Madajewski B, Zanzonico P, Sequeira S, Gonen M, Wiesner U, Bradbury MS, Target-or-clear zirconium-89 labeled silica nanoparticles for enhanced cancer-directed uptake in melanoma: a comparison of radiolabeling strategies, Chem. Mater. 29 (2017) 8269–8281, 10.1021/acs.chemmater.7b02567. [PubMed: 29123332]

[159]. Chen F, Zhang X, Ma K, Madajewski B, Benezra M, Zhang L, Phillips E, Turker MZ, Gallazzi F, Penate-Medina O, Overholtzer M, Pauliah M, Gonen M, Zanzonico P, Wiesner U, Bradbury MS, Quinn TP, Melanocortin-1 receptor-targeting ultrasmall silica nanoparticles for dual-modality human melanoma imaging, ACS Appl. Mater. Interfaces 10 (2018) 4379–4393, 10.1021/acsami.7b14362. [PubMed: 29058865]

[160]. Chen F, Madajewski B, Ma K, Zhang L, Zanzonico P, Quinn T, Wiesner U, Bradbury M, Renally clearable PSMA inhibitors conjugated ultrasmall silica nanoparticles enhance the specific detection of prostate cancer in vivo, J. Nucl. Med. 59 (2018) (467–467).

[161]. Chen F, Ma K, Madajewski B, Zhuang L, Zhang L, Rickert K, Marelli M, Yoo B, Turker MZ, Overholtzer M, Quinn TP, Gonen M, Zanzonico P, Tuesca A, Bowen MA, Norton L, Subramony JA, Wiesner U, Bradbury MS, Ultrasmall targeted nanoparticles with engineered antibody fragments for imaging detection of HER2-overexpressing breast cancer, Nat. Commun. 9 (2018) 4141, 10.1038/s41467-018-06271-5. [PubMed: 30297810]

[162]. Fu Y, Li X, Chen H, Wang Z, Yang W, Zhang H, CXC chemokine receptor 4 antagonist functionalized renal clearable manganese-doped iron oxide nanoparticles for active-tumor-targeting magnetic resonance imaging-guided bio-photothermal therapy, ACS Appl. Bio Mater. 2 (2019) 3613–3621, 10.1021/acsabm.9b00475.

[163]. Yu M, Zhou C, Liu L, Zhang S, Sun S, Hankins JD, Sun X, Zheng J, Interactions of renal-clearable gold nanoparticles with tumor microenvironments: vasculature and acidity effects, Angew. Chem. Int. Ed. 56 (2017) 4314–4319, 10.1002/anie.201612647.

[164]. Choi HS, Kang H, El Fakhri G, Renal Clearable Organic Nanocarriers, in, US Patent App. 16/314,149, 2019.

Author Manuscript Author Manuscript Author Manuscript Author Manuscript

[165]. Madajewski B, Chen F, Yoo B, Ma K, Turker M, Zhang L, Zanzonico P, Wiesner U, Bradbury M, Ultrasmall silica nanoparticle platforms for improved small molecular inhibitor delivery and efficacy, J. Nucl. Med. 60 (2019) (278–278).

[166]. Bradbury MS, Yoo B, Wiesner U, Ma K, Nanoparticle Drug Conjugates, in, US Patent App. 16/137,709, 2019.

[167]. Juthani R, Madajewski B, Yoo B, Zhang L, Chen P-M, Chen F, Turker MZ, Ma K, Overholtzer M, Longo VA, Carlin S, Aragon-Sanabria V, Huse JT, Gonen M, Zanzonico PB, Rudin CM, Wiesner U, Bradbury MS, Brennan CW, Ultrasmall core-shell silica nanoparticles for precision drug delivery in a high-grade malignant brain tumor model, Clin. Cancer Res. (2019), 10.1158/1078-0432.ccr-19-1834 (clincanres.1834.2019).

[168]. Thomas E, Colombeau L, Gries M, Peterlini T, Mathieu C, Thomas N, Boura C, Frochot C, Vanderesse R, Lux F, Ultrasmall AGuIX theranostic nanoparticles for vascular-targeted interstitial photodynamic therapy of glioblastoma, Int. J. Nanomedicine 12 (2017) 7075. [PubMed: 29026302]

[169]. Detappe A, Kunjachan S, Rottmann J, Robar J, Tsiamas P, Korideck H, Tillement O, Berbeco R, AGuIX nanoparticles as a promising platform for image-guided radiation therapy, Cancer Nanotechnol. 6 (2015) 4, 10.1186/s12645-015-0012-3. [PubMed: 26345984]

[170]. Kim SE, Zhang L, Ma K, Riegman M, Chen F, Ingold I, Conrad M, Turker MZ, Gao M, Jiang X, Monette S, Pauliah M, Gonen M, Zanzonico P, Quinn T, Wiesner U, Bradbury MS, Overholtzer M, Ultrasmall nanoparticles induce ferroptosis in nutrient-deprived cancer cells and suppress tumour growth, Nat. Nanotechnol. 11 (2016) 977, 10.1038/nnano.2016.164. [PubMed: 27668796]

[171]. Albanese A, Lam AK, Sykes EA, Rocheleau JV, Chan WCW, Tumour-on-a-chip provides an optical window into nanoparticle tissue transport, Nat. Commun. 4 (2013) 2718, 10.1038/ncomms3718. [PubMed: 24177351]

[172]. Bugno J, Poellmann MJ, Sokolowski K, Hsu H.-j., Kim D-H, Hong S, Tumor penetration of Sub-10 nm nanoparticles: effect of dendrimer properties on their penetration in multicellular tumor spheroids, nanomedicine: nanotechnology, Biol. Med. 21 (2019) 102059, 10.1016/j.nano.2019.102059.

[173]. Peng C, Gao X, Xu J, Du B, Ning X, Tang S, Bachoo RM, Yu M, Ge W-P, Zheng J, Targeting orthotopic gliomas with renal-clearable luminescent gold nanoparticles, Nano Res. 10 (2017) 1366–1376, 10.1007/s12274-017-1472-z. [PubMed: 29034063]

[174]. Jiang X, Du B, Zheng J, Glutathione-mediated biotransformation in the liver modulates nanoparticle transport, Nat. Nanotechnol. 14 (2019) 874–882, 10.1038/s41565-019-0499-6. [PubMed: 31308501]

[175]. Vinluan RD, Yu M, Gannaway M, Sullins J, Xu J, Zheng J, Labeling monomeric insulin with renal-clearable luminescent gold nanoparticles, Bioconjug. Chem. 26 (2015) 2435–2441, 10.1021/acs.bioconjchem.5b00490. [PubMed: 26465678]

[176]. Riley RS, June CH, Langer R, Mitchell MJ, Delivery technologies for cancer immunotherapy, Nat. Rev. Drug Discov. 18 (2019) 175–196, 10.1038/s41573-018-0006-z. [PubMed: 30622344]

[177]. Zhang Y-N, Lazarovits J, Poon W, Ouyang B, Nguyen LNM, Kingston BR, Chan WCW, Nanoparticle size influences antigen retention and presentation in lymph node follicles for humoral immunity, Nano Lett. 19 (2019) 7226–7235, 10.1021/acs.nanolett.9b02834. [PubMed: 31508968]

[178]. Ju E, Li T, Ramos da Silva S., Gao S-J, Gold nanocluster-mediated efficient delivery of Cas9 protein through pH-induced assembly-disassembly for inactivation of virus oncogenes, ACS Appl. Mater. Interfaces 11 (2019) 34717–34724, 10.1021/acsami.9b12335. [PubMed: 31469541]

[179]. Du B, Jiang X, Das A, Zhou Q, Yu M, Jin R, Zheng J, Glomerular barrier behaves as an atomically precise bandpass filter in a sub-nanometre regime, Nat. Nanotechnol. 12 (2017) 1096, 10.1038/nnano.2017.170. [PubMed: 28892099]

[180]. Leong HS, Butler KS, Brinker CJ, Azzawi M, Conlan S, Dufés C, Owen A, Rannard S, Scott C, Chen C, Dobrovolskaia MA, Kozlov SV, Prina-Mello A, Schmid R, Wick P, Caputo F, Boisseau P, Crist RM, McNeil SE, Fadeel B, Tran L, Hansen SF, Hartmann NB, Clausen LPW, Skjolding LM, Baun A, Ågerstrand M, Gu Z, Lamprou DA, Hoskins C, Huang L, Song W, Cao H, Liu X, Jandt KD, Jiang W, Kim BYS, Wheeler KE, Chetwynd AJ, Lynch I, Moghimi SM, Nel A, Xia T,

Author Manuscript Author Manuscript Author Manuscript Author Manuscript

Weiss PS, Sarmento B, das Neves J, Santos HA, Santos L, Mitragotri S, Little S, Peer D, Amiji MM, Alonso MJ, Petri-Fink A, Balog S, Lee A, Drasler B, Rothen-Rutishauser B, Wilhelm S, Acar H, Harrison RG, Mao C, Mukherjee P, Ramesh R, McNally LR, Busatto S, Wolfram J, Bergese P, Ferrari M, Fang RH, Zhang L, Zheng J, Peng C, Du B, Yu M, Charron DM, Zheng G, Pastore C, On the issue of transparency and reproducibility in nanomedicine, Nat. Nanotechnol. 14 (2019) 629–635, 10.1038/s41565-019-0496-9. [PubMed: 31270452]

Author Manuscript Author Manuscript Author Manuscript Author Manuscript

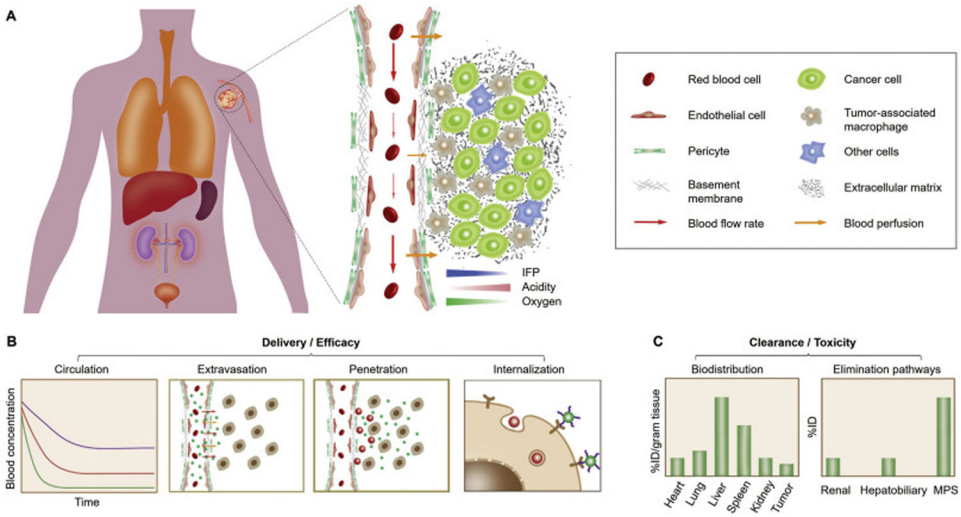

Fig. 1.

In vivo delivery and clearance of cancer nanomedicines. (A) For effective tumor targeting and delivery, the administrated nanomedicines generally take a sequential in vivo transport route, including circulation in bloodstream, extravasation across tumor vasculature, penetration within tumor interstitium to cancer cells, and cell internalization. However, a series of physiological barriers may considerably impair the therapeutic outcome of engineered nanomedicines: 1) During blood circulation, DDSs may be immediately sequestered by the mononuclear phagocyte system (MPS), resulting in shortened blood retention; 2) Subsequently, DDS extravasation across abnormal tumor vasculature is impeded by the high interstitial fluid pressure (IFP) and poor blood perfusion in tumor microenvironment (TME); 3) Next, intratumoral penetration of DDSs can be further limited due to the presence of dense extracellular matrix (ECM) and tumor-associated macrophages (TAMs); 4) Eventually, cell internalization of DDSs will be affected by their affinity not only to cancer cells but also to neighboring non-cancer cells. (B) Therapeutic efficacy of administrated nanomedicines is closely related to their delivery effectiveness to the population of cancer cells in tumor. Therefore, strategic design of nanomedicines is required to successfully overcome these physiological barriers along the in vivo transport route. (C) Meanwhile, toxicity of the administrated nanomedicines is largely affected by the different elimination pathways as well as the biodistribution and retention in normal tissues.

Author Manuscript Author Manuscript Author Manuscript Author Manuscript

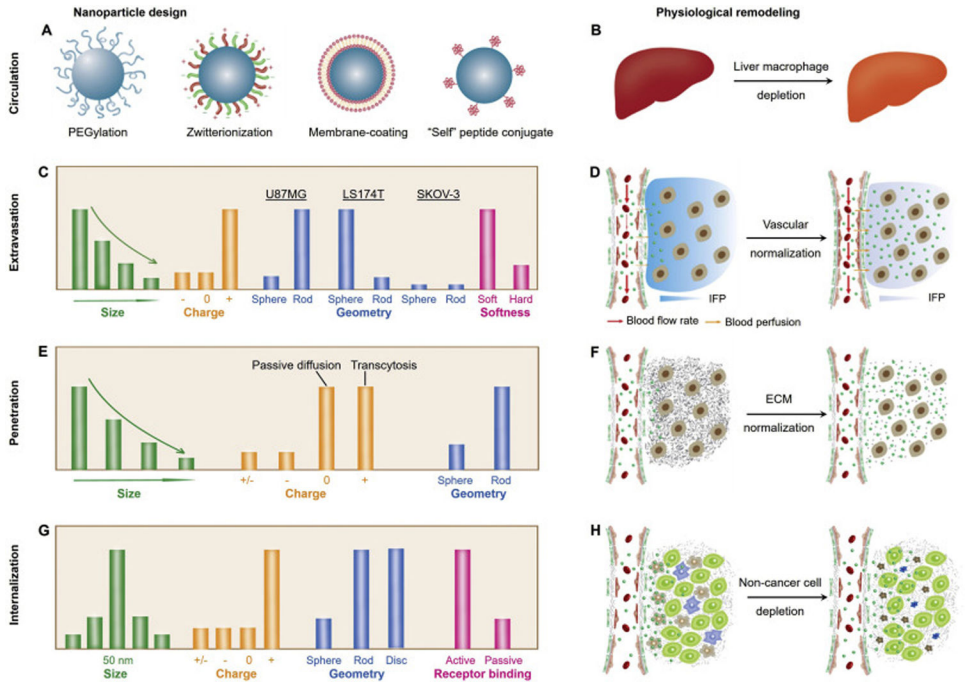

Fig. 2.

Emerging delivery strategies for various cancer nanomedicines. During the past years, many breakthroughs have been achieved in understanding the physiological barriers and developing novel delivery strategies (in nanoparticle design and physiological remodeling). (A-B) During the blood circulation, the MPS serves as one of the most important barriers for drug delivery, therefore, many strategies have been applied or proposed to escape the MPS uptake and to prolong blood circulation, including surface modification of nanomedicines (A) and depletion of liver macrophages (B). (C-D) Throughout the past decades, various physicochemical properties of NPs have been investigated to increase the vascular permeability of NPs (through EPR-based extravasation or transendothelial transport, C), whereas, normalization of tumor vasculature may also serve as a viable approach to increase the efficacy of nanomedicines (D). (E-F) The nanoparticle penetration in TME can be improved by tuning the physicochemical properties of NPs to facilitate passive diffusion or transcytosis (E) as well as by the normalization of dense and disorganized ECM (F). (G-H) After successfully overcoming the proceeding barriers, the nanomedicines that are intended for active targeting will still need to interact with cancer cells for internalization. Some strategies to potentially address this challenge includes rational nanoparticle design (in size, charge, geometry and surface conjugation, G) as well as the depletion of non-cancer cells (such as tumor-associated macrophages and fibroblasts, H).

Author Manuscript Author Manuscript Author Manuscript Author Manuscript

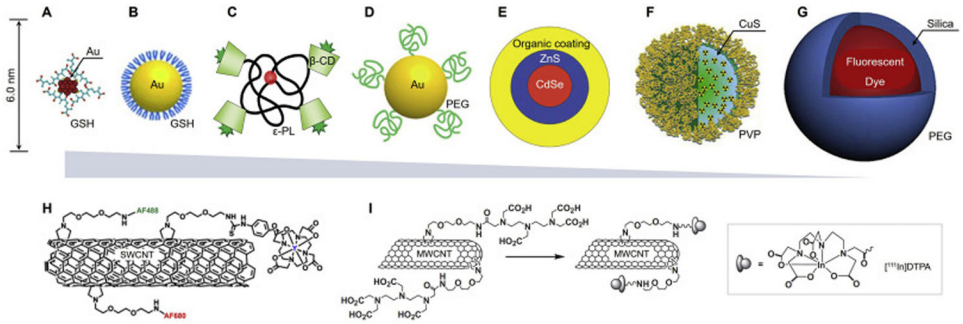

Fig. 3.

Representative engineered renal clearable NPs of various sizes and compositions. (A) Zwitterionic glutathione (GSH)-coated gold nanoclusters ($Au_{25}SG_{18}$, ~2 nm), ref. [128,174]. (B) Zwitterionic GSH-coated gold nanoparticles (GS-AuNPs, 3.3 nm), ref. [149]. (C) Organic β-cyclodextrin (β-CD)-ε-polylysine (εPL) NPs (H-dots, CDPL NPs, 4.6–4.9 nm), ref. [53]. (D) PEGylated AuNPs (PEG-AuNPs, 5.5 nm), ref. [51]. (E) Zwitterionic CdSe/ZnS quantum dots (QDs, 4.4–8.7 nm), ref. [9]. (F) Polyvinylpyrrolidone (PVP)-coated copper sulfide nanodots (CuS NDs, 5.6 nm), ref. [136]. (G) PEGylated core-shell silica-based NPs (C-dots and C′-dots, ~7 nm), ref. [127,152]. The sizes in (A-G) are reported in hydrodynamic diameter (HD). (H-I) In addition to the ultrasmall NPs (A-G), small-molecule probes and biodegradable nanomaterials, some large nanomaterials have also been reported to be renally clearable, such as single-walled carbon nanotubes (SWCNTs, average length 200–300 nm, diameter 0.8–1.2 nm, H, ref. [129]) and multi-walled carbon nanotubes (MWCNTs, length 0.5–2.0 μm, diameter 20–30 nm, I, ref. [148]). (For interpretation of the references to colour in this figure legend, the reader is referred to the web version of this article.)

Author Manuscript Author Manuscript Author Manuscript Author Manuscript

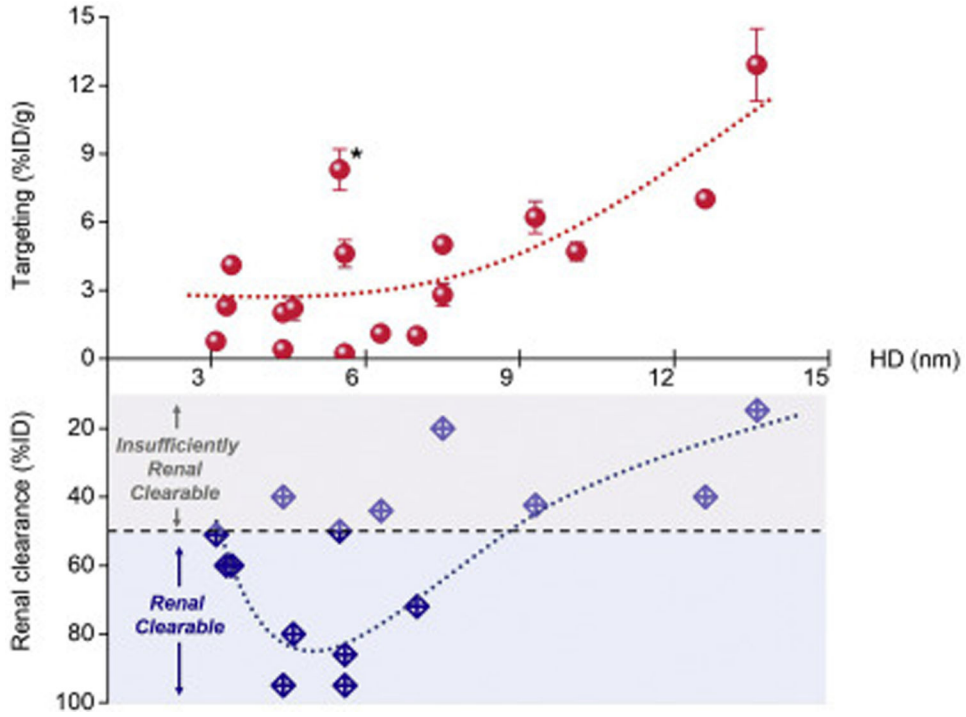

Fig. 4.

Tumor targeting (passive) and renal clearance of renal clearable NPs with different sizes. The NP size, renal clearance and targeting efficiency, were plotted from the data sets in Table S1 in supplementary information. As a result, the NPs with more efficient renal clearance (> 80%ID) would generally have lower targeting efficiency (< 3%ID/g). Meanwhile, the renal clearable PEG-AuNPs (asterisk (*) in the figure) were found to have higher tumor targeting efficiency compared to other NPs of similar sizes, which might be due to the density-dependent margination effect in tumor blood flow and resulting enhanced NP extravasation, ref. [156]. To be noted, the renal clearance efficiencies were mainly quantified based on the recovery percentages (ranging from 24 to 168 h post-injection) of the administrated NPs in urine from the reports; the targeting efficiencies were analyzed as the NP accumulation in tumor at selected time points (at least 6 h post-injection) from the reports.

Author Manuscript Author Manuscript Author Manuscript Author Manuscript

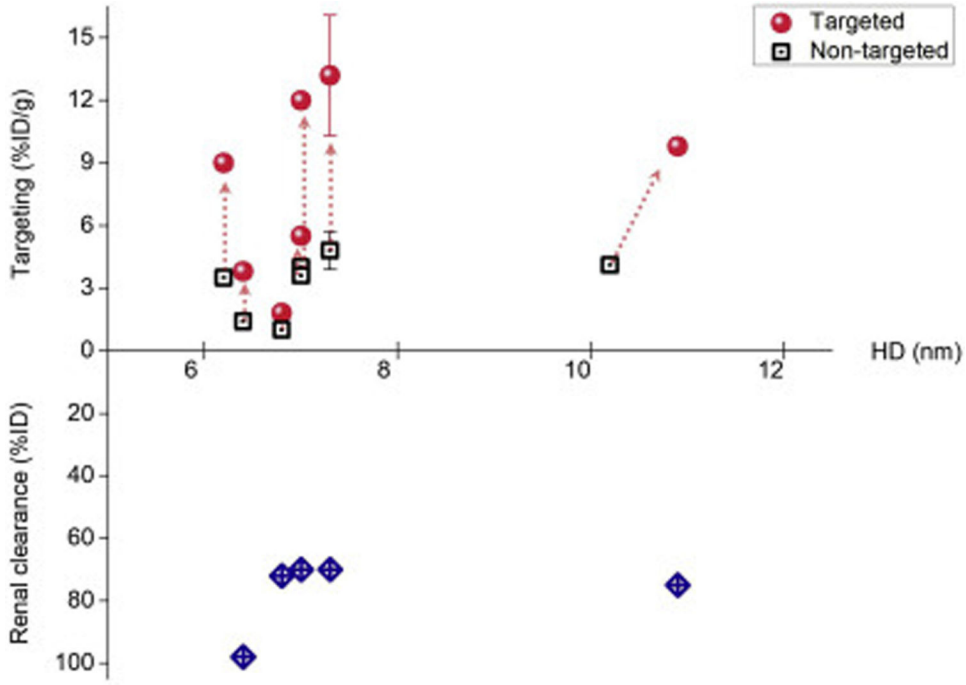

Fig. 5.

Tumor targeting (active) and renal clearance of renal clearable NPs with different sizes. The NP size, renal clearance and targeting efficiency were plotted from the data sets in Table S2 in supplementary information. As shown above, the renal clearable NPs (i.e., C-dots) could achieve much higher targeting efficiency (2.6-fold increase, median) among many cancer types by the targeted strategy compared to non-targeted ones. This would allow for the both enhanced tumor targeting and body elimination.

Author Manuscript Author Manuscript Author Manuscript Author Manuscript

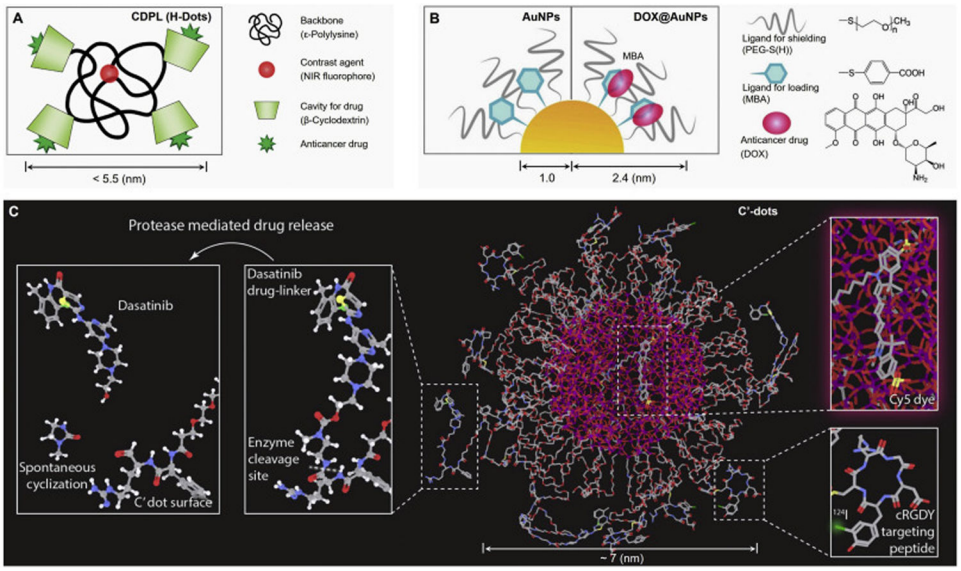

Fig. 6.

Representative renal clearable NP-based DDSs. (A) Renal clearable organic nanocarriers (H-Dots, CDPL, < 5.5 nm) in the proposed loading (within the β-CD cavity) and delivery of anticancer drugs, ref. [53]. (B) Renal clearable AuNP-based DDS (DOX@AuNPs, 4.8 nm) in the loading (via π-π stacking and PEG shielding) and delivery of the small-molecule drug, doxorubicin (DOX), ref. [151]. (C) Pegylated ultrasmall silica NPs (C′-dots, ~7 nm) in the conjugation and delivery of small molecular inhibitors (SMIs) such as dasatinib and gefitinib, ref. [165,167].

Author Manuscript Author Manuscript Author Manuscript Author Manuscript

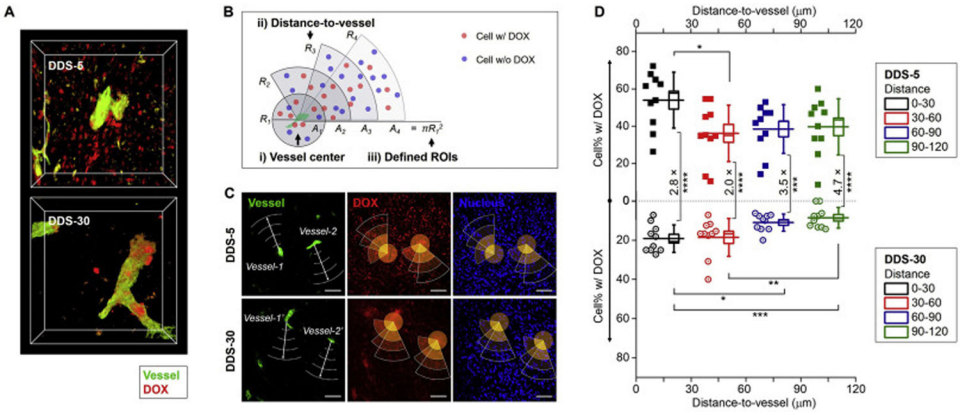

Fig. 7.

Enhanced vascular permeability and intratumoral drug delivery of renal clearable AuNP-based DDS. (A) From the confocal microscopy imaging, renal clearable DDS-5 showed increased tumor accumulation and intratumoral diffusion in TME compared with non-renal clearable DDS-30 within 12 h post-injection. (B-D) With the quantitative analysis of cell percentage (cell%) interacting with DOX across different distances from tumor blood vessels, renal clearable DDS-5 showed much greater accumulation and deeper penetration versus non-renal clearable DDS-30. This was primarily due to the unique strengths of the DDS-5, the ultrasmall size and ultrahigh vascular permeability, for the rapid tumor targeting and efficient drug delivery, ref. [119].

Author Manuscript Author Manuscript Author Manuscript Author Manuscript

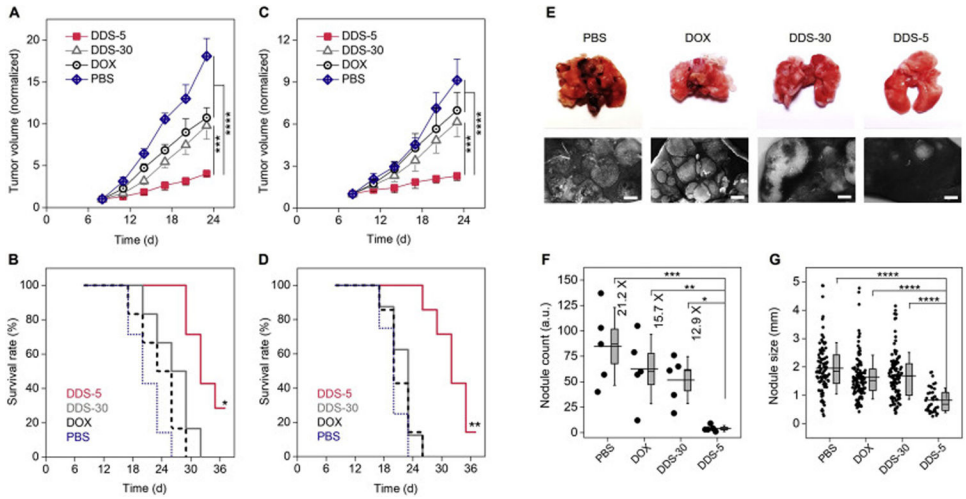

Fig. 8.

Improved antitumor efficacy of renal clearable DDS among primary and metastatic tumor models. (A-D) Normalized tumor growth curves and survival rates of the MCF-7 xenograft (A, B) and 4T1 primary (C, D) tumors, respectively, during the successive treatments. For A and C, ***P < .0005, ****P < .0001 (One-Way ANOVA, n = 5). For B, *indicates P < .05, < 0.005, < 0.0005 for DDS-5 versus DDS-30, free DOX and PBS, respectively; For D, **indicates P < .001 for DDS-5 versus DDS-30 and free DOX, P < .0005 for DDS-5 versus PBS, respectively (Kaplan-Meier, n = 6–8). (E) Images of mice lungs after the successive treatments (day-23). Scale bar, 1 mm. (F) Nodule counts of the metastatic lung tumors after treatments. *P < .05, **P < .01, ***P < .001, ****P < .0001. Box indicates median and s.e.m. (G) Lung tumor nodule sizes. ****P < .0001. Box indicates median and 25–75% interquartile range (n = 5). Adapted from ref. [119,151].

Author Manuscript Author Manuscript Author Manuscript Author Manuscript

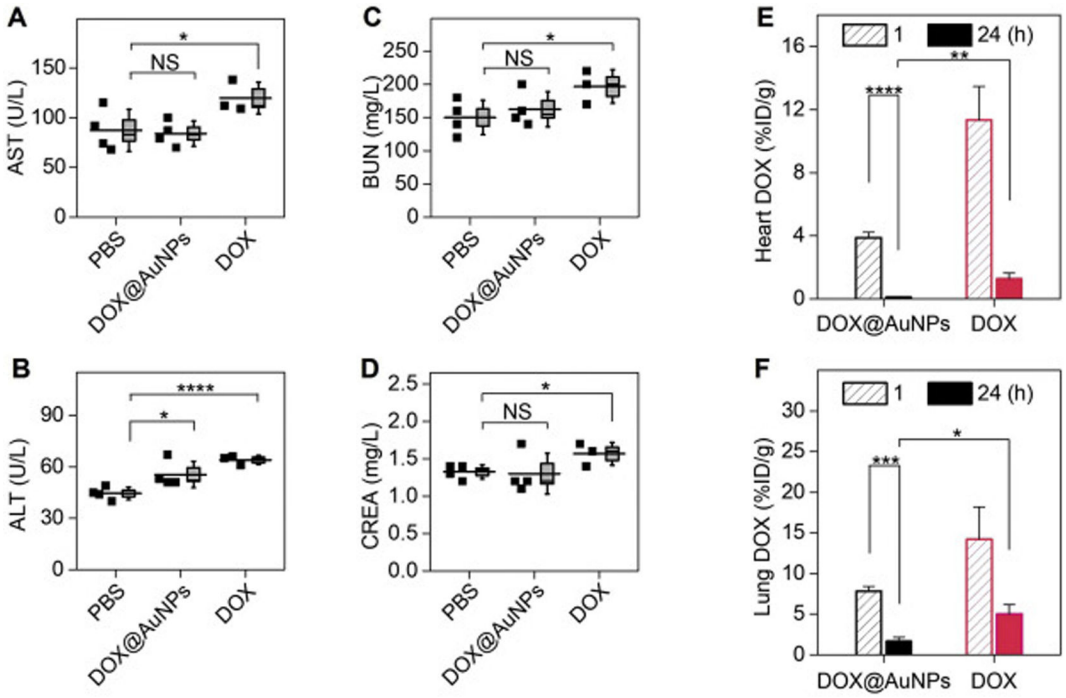

Fig. 9.

Minimized toxicity of loaded drug (DOX) using renal clearable nanocarriers. (A-D) Blood chemistry analysis after successive treatments, suggesting the renal clearable DDS (DOX@AuNPs) can minimize the impairment of DOX to liver and kidney functions. Aspartate transaminase, AST (A), alanine aminotransferase, ALT (B), blood urea nitrogen, BUN (C), creatinine, CREA (D). $*P < .05$, $****P < .0001$, NS, not significant ($n = 4$ for DOX@AuNPs and PBS; $n = 3$ for free DOX, where one animal died during study). (E-F) DOX biodistribution study, showing renal clearable nanocarriers can significantly minimize the drug accumulation and retention in vital organs, including heart (E) and lungs (G) ($n = 3$). $*P < .05$, $**P < .01$, $***P < .005$, $****P < .0001$ (Student's *t*-test). Adapted from ref. [151].

Author Manuscript Author Manuscript Author Manuscript Author Manuscript

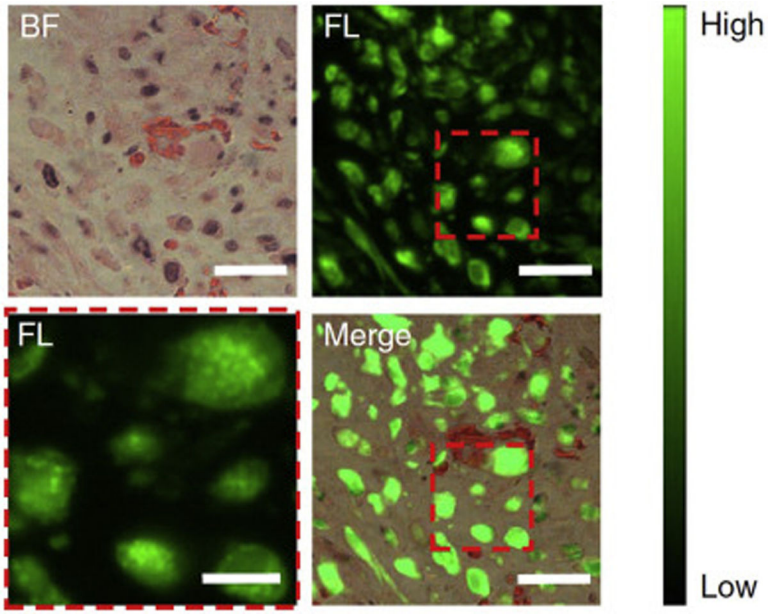

Fig. 10.

Enhanced intratumoral delivery of molecular probes (ICG) using renal clearable nanocarriers. From tumor fluorescence imaging with 24 h post-intravenous treatment of ICG_4-GS-Au_{25}, ICG (green) was efficiently taken up by tumor cells and located in endosome-like membrane-bound compartments (lower left, enlarged view), indicating the renal clearable nanocarriers, AuNCs, effectively deliver these molecular probes into tumor sites, ref. [174]. BF, bright field, FL, fluorescence; Scale bars, 6 μm for the enlarged view lower left and 20 μm for the rest. (For interpretation of the references to colour in this figure legend, the reader is referred to the web version of this article.)

Author Manuscript Author Manuscript Author Manuscript Author Manuscript

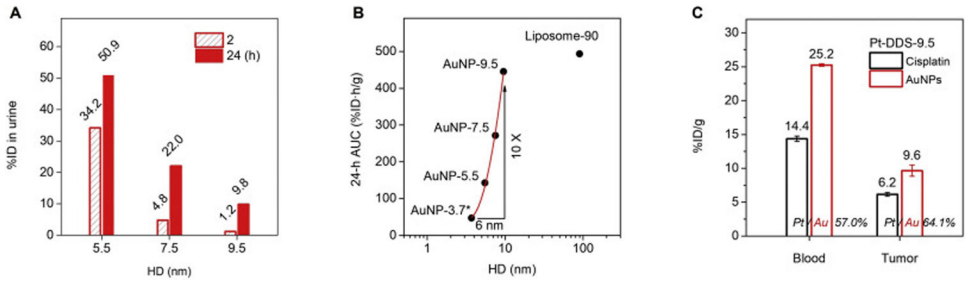

Fig. 11.

Precise tuning of renal clearance, pharmacokinetics and tumor targeting with renal clearable DDSs. (A) The size of ultrasmall AuNP-based nanocarriers can be precisely tuned near or above the KFT (5–10 nm), so that the renal clearance efficiency can be decreased (from 50% to 10% ID, for AuNPs from 5.5 nm to 9.5 nm) for longer blood circulation. The AuNPs of 5.5, 7.5 and 9.5 nm were prepared with different core size and the same PEG surface coating (PEG 800 Da). The renal clearance was collected as the average of three mice. (B) As a result, the blood circulation of these nanocarriers (in terms of 24-h AUC, see Table. S3 for pharmacokinetic parameters) can be increased by 10 times or 1 order of magnitude within the 6 nm size window, which allows for the prolonged blood retention of the 9.5 nm AuNPs (AuNP-9.5) to be comparable with that of 90 nm PEGylated liposome (Liposome-90). (C) Due to the improved blood circulation, the 9.5 nm cisplatin-loaded AuNP-based DDS (Pt-DDS-9.5) can achieve 25.2%ID/g AuNPs and 14.4%ID loaded cisplatin concentrations in blood at 12 h post-intravenous injection. More importantly, this ultrasmall DDS with ultrahigh vascular permeability enables the significant tumor accumulation of not only the delivery vector but also the loaded drug (in 4T1 tumor model, $n = 3$).

Author Manuscript Author Manuscript Author Manuscript Author Manuscript

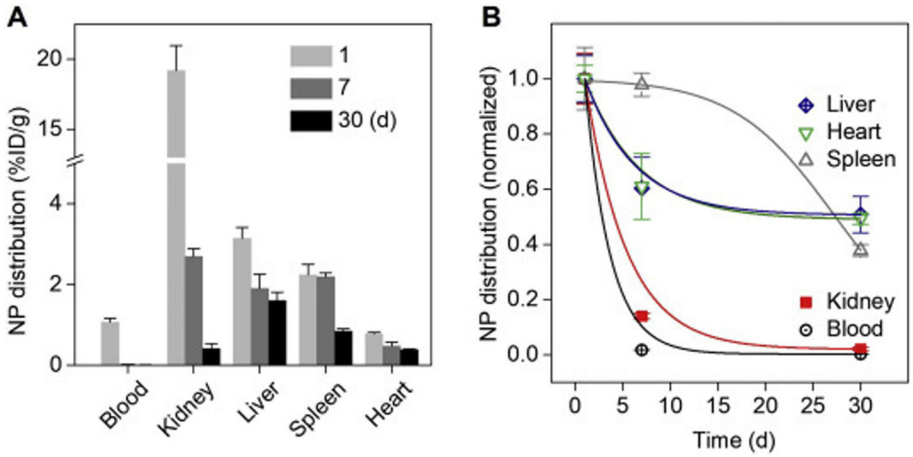

Fig. 12.

Distribution and elimination of renal clearable nanocarriers (AuNPs) in blood and vital organs. (A) Distribution of the renal clearable nanocarrier, AuNPs, in both blood and the vital organs (kidney, liver, spleen, and heart) on 1, 7 and 30 d post-intravenous injection (n = 3). (B) Normalized distribution and elimination kinetics of renal clearable AuNPs within 30 d. Compared with blood and other organs, the kidney showed one of the fastest clearance rates of renal clearable AuNPs within 30 d.